eLife

Reviewed Preprint
v2 • October 14, 2024
Revised by authors

Reviewed Preprint
v1 • March 13, 2024

Neuroscience

Gliogenesis from the subventricular zone modulates the extracellular matrix at the glial scar after brain ischemia

Maria Ardaya, Marie-Catherine Tiveron, Harold Cremer, Benjamin Dehay, Fernando Pérez-Cerdá, Carlos Matute, Federico N Soria, Fabio Cavaliere

Achucarro Basque Center for Neuroscience, Leioa, Spain • Department of Neuroscience, University of the Basque Country (UPV/EHU), Leioa, Spain • CIBERNED, Madrid, Spain • Donostia International Physics Center (DIPC), San Sebastian, Spain • Aix Marseille Univ, CNRS, IBDM, Campus de Luminy, Marseille, France • Univ. Bordeaux, CNRS, IMN, UMR 5293, Bordeaux, France • Ikerbasque, Basque Foundation for Science, Bilbao, Spain • Basque Biomodel Platform for Human Research (BBioH), Leioa, Spain • Instituto Biofisika (CSIC, UPV/EHU), Fundación Biofísica Bizkaia, Leioa, Spain

Abstract

Activation of the subventricular zone (SVZ) following cerebral ischemia is one of the brain's early responses to counteract neuron loss and minimize tissue damage. Impaired brain regions communicate with the SVZ through various chemotactic signals that promote cell migration and differentiation, primarily involving neural stem cells (NSC), neuroblasts, or glioblasts. However, the activation of gliogenesis and the role of newly formed astrocytes in the post-ischemic scenario remain subjects of debate. We have previously demonstrated that adenosine release after brain ischemia prompts the SVZ to generate new astrocytes. Here, we used transient brain ischemia in mice to identify the cellular origin of these astrocytes within the SVZ neurogenic niche and to investigate their role in the pathological process. By combining immunofluorescence, BrdU-tracing, and genetic cell labeling, we tracked the migration of newborn astrocytes, positive for the proteoglycan marker Thbs4, from the dorsal and medial SVZ to the perilesional barrier surrounding the ischemic core, known as the "glial scar". We found that these Thbs4-positive astrocytes modulate the dense extracellular matrix at the lesion border by both synthesizing and degrading hyaluronan. We also show that while the accumulation of this polymer at the lesion site is sufficient to recruit newborn astrocytes, its degradation at the SVZ correlates with gliogenesis. These findings suggest that newborn astrocytes could be a promising pharmacological target for modulating the glial scar after brain ischemia and facilitate tissue regeneration.

eLife Assessment

This work shows that newborn Thbs4-positive astrocytes generated in the adult subventricular zone (SVZ) respond to middle carotid artery occlusion (MCAO) by secreting hyaluronan at the lesion penumbra, and that hyaluronin is a chemoattractant to SVZ astrocytes. These findings are **important**, despite mostly descriptive, as they point to a relevant function of SVZ newborn astrocytes in the modulation of the glial scar after brain ischemia. The methods, data and analyses are **convincing** and broadly support the claims made by the authors with only some weaknesses.

https://doi.org/10.7554/eLife.96076.2.sa3

Introduction

Cell regeneration in the adult mammalian brain primarily occurs mainly in two neurogenic niches: the subventricular zone (SVZ) in the lateral ventricle and the subgranular zone (SGZ) in the dentate gyrus of the hippocampus (Bond et al., 2015). Adult brain stem cells are multipotent and originate from the embryonic radial glia, thus sharing **key** cell markers and features with resident astrocytes. In the adult mouse brain, neuroblasts from SVZ migrate through the rostral migratory stream (RMS) to the olfactory bulb (OB), where neurogenesis takes place (Luskin, 1993). Neuronal hyperactivity (e.g., during epilepsy), as well as pathological conditions (e.g., stroke) or natural (e.g., aging) processes, can impair the physiological functions of the neurogenic niches, altering their neurogenic and gliogenic potential (Chaker et al., 2016; Kralic et al., 2005; Sundholm-Peters et al., 2005). For instance, it is known that SVZ cells are activated *in vivo* after focal ischemia following a middle cerebral artery occlusion (MCAO) (Ceanga et al., 2021).

We have previously demonstrated in oxygen and glucose-deprived (OGD) organotypic brain slices that the ischemic region and the SVZ establish a biochemical interplay based on a gradient of toxic and protective factors released early after the insult (Cavaliere et al., 2006). Furthermore, others have demonstrated that brain stroke models in mice can activate astrogliogenesis at the expense of neurogenesis (Benner et al., 2013; Laug et al., 2019; Li et al., 2010). Benner and colleagues identified a SVZ-derived astrocyte population characterized by high levels of the membrane-bound proteoglycan thrombospondin 4 (Thbs4), a cell-cell and cell-matrix adhesion molecule that has been considered neuroprotective against ischemic damage (Benner et al., 2013; Laug et al., 2019). Ablation of Thbs4 in KO mice also produced abnormal ischemic scar formation and increased microvascular hemorrhage, suggesting a role of SVZ astrogliogenesis in brain damage and glial scar formation induced by ischemic stroke (Benner et al., 2013).

The perilesional barrier known as the *glial scar* assembles early after brain ischemia, isolating the damaged area and limiting both the spread of pathogens and potentially toxic damage-associated molecular patterns (DAMPs) into the surrounding area (Anderson et al., 2016; Bush et al., 1999; Faulkner et al., 2004). Consisting of packed reactive astrocytes and a dense extracellular matrix composed mostly of hyaluronic acid (HA), the glial scar represents a physical barrier for the SVZ-generated newborn neurons that migrate into the ischemic core (Arvidsson et al., 2002; Yamashita et al., 2006). Thus, modulating glial scar formation after brain ischemia may be a strategy to reduce tissue damage and restore brain functionality. In ischemic stroke, the brain extracellular matrix (ECM) goes through a significant reorganization due to injury and must undergo successful remodeling to promote brain repair. ECM elements involved in the ischemic cascade induce activation of astrocytes and microglia, which modulate ECM structure by releasing

glycoproteins into the extracellular space (Adams and Gallo, 2018; Fawcett, 2015). This crosstalk culminates in the formation of the glial scar, which is created locally by reactive astrocytes and astrocytes-secreted ECM molecules such as HA and chondroitin sulphate proteoglycans (Bush et al., 1999; Lau et al., 2013).

We have previously demonstrated that high extracellular adenosine levels, a hallmark of ischemic insults, induce astrogliogenesis from the SVZ (Benito-Muñoz et al., 2016). Following our previous results, here we characterize the SVZ response to brain ischemia and investigate the role of newly generated astrocytes in the modulation of the glial scar after MCAO. We show that ischemic conditions increase the number of newly generated astrocytes in the SVZ and their migration to the ischemic area. We also propose the role of these astrocytes in modulating the extracellular matrix at the glial scar and suggest this astrocyte population as a possible target for brain repair after brain ischemia.

Results

Thbs4 is expressed in the neurogenic niche of the SVZ

As suggested by others (Benner et al., 2013; Girard et al., 2014; Pous et al., 2020), Thbs4 is highly expressed in astrocytes of the SVZ and RMS and might play a role in ischemia-induced neurogenesis. To confirm these observations, we labeled the mouse SVZ by immunofluorescence for Thbs4. Thbs4 was mainly expressed in the SVZ, RMS, and OB but also in the cerebellum and ventral tegmental area (**Fig. 1A**). In the SVZ, the staining was associated with cells with different morphologies (**Fig. 1B**), ranging from cells with small primary apical processes in contact with the ventricle, to rounded NSC-like cells in the dorsolateral SVZ horn. After quantification by direct count of Thbs4-positive cells, Thbs4-positive astrocytes represented 21.4% of the total SVZ cells (**Fig. 1C**), with more than 60% of them displaying a radial glia-like type-B morphology (Bond et al., 2015; Doetsch et al., 1999) (**Fig. 1D**). This is in accordance with other studies reporting Thbs4 expression in B-cells, either by immunohistochemistry (Beckervordersandforth et al., 2010; Benner et al., 2013) or single-cell RNA sequencing (Basak et al., 2018; Cebrian-Silla et al., 2021; Llorens-Bobadilla et al., 2015).

To validate the immunohistochemistry protocol for Thbs4, we labeled the SVZ cells with green fluorescent protein (GFP) under the control of the Thbs4 promoter (pThbs4-eGFP) by postnatal (P1) electroporation (**Fig. 1E**). Twenty-four hours after electroporation, almost 20% of total cells in the dorsal SVZ expressed GFP (**Fig. 1F**), with a greater expression in the rostral SVZ (**Fig. 1G**), confirming that Thbs4-positive cells were mainly localized in the neurogenic niche of the SVZ. This also suggests that Thbs4 is expressed in NSCs at early postnatal stages, generating astrocytes alongside development.

Thbs4 expression in the SVZ increases after brain ischemia

To investigate whether brain ischemia could activate astrogliogenesis in the SVZ, we analyzed cell proliferation and Thbs4 expression in the SVZ after MCAO. Sixty minutes of MCAO (**Fig. S1A**) caused neuronal damage in the cortex and striatum, as observed by cresyl violet staining (**Fig. S1B**) and NeuN immunofluorescence (**Fig. S1C**). The survival rate at 28 days post-lesion was around 50% (**Fig. S1D**). Moreover, motor deficits and animal weight of ischemic mice were monitored every day after MCAO for 30 days. Motor deficits improved overtime, while body weight dropped sharply the first 3 days after MCAO and was partially restored at 30 dpi (**Fig. S1E-F**).

To study cell proliferation in the SVZ, we administered 50 mg/kg BrdU i.p. every two hours (3 doses in total) the day before MCAO (**Fig. S2A**). We observed an increase in the number of total SVZ BrdU-positive cells 24h after MCAO (**Fig. S2B-C**). Ki67 immunofluorescence of SVZ wholemount

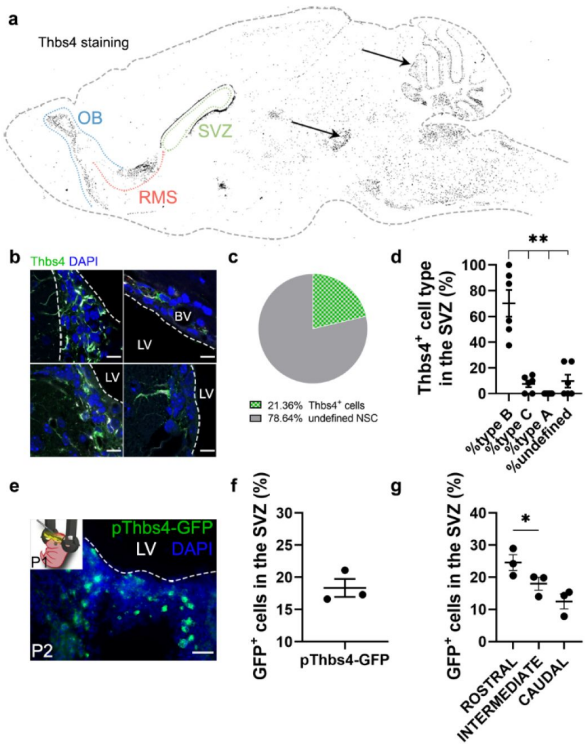

Figure 1

Thbs4 labels type-B cells in the SVZ neurogenic niche.

(a) Schematic drawing of the brain showing Thbs4 labeling throughout the mouse brain. Thbs4 was primarily found in the SVZ and RMS of the adult mouse telencephalon. Arrows indicate non-specific Thbs4 staining in cerebellum and ventral tegmental area. (b) Thbs4 positive cells in the SVZ displayed various morphologies. (c) Proportion of Thbs4-positive cells relative to the total NSCs population in the SVZ. (d) Classification of Thbs4-positive cells in the SVZ based to their NSC morphology. (e) Electroporation of pThbs4-GFP at P1 revealed Thbs4 expression in the postnatal dorsal SVZ. (f) Quantification of Thbs4-reporter expression showing the proportion of NSC expressing Thbs4 postnatally in the dorsal SVZ. (g) Thbs4-GFP reporter expression was upregulated in the rostral SVZ. BV: Blood vessel; LV: Lateral ventricle. Scale bar = 10 μm (b) and 50 μm (e). Bars represent mean ± SEM. *$p < 0.05$ and **$p < 0.01$, Tukey post hoc test (after one-way ANOVA was significant at $p < 0.05$).

preparations (**Fig. S2D**) also revealed a more than tenfold increase of proliferative cells 24h after MCAO (**Fig. S2E**). In addition, we observed a significant increase in cleaved Caspase3-positive cells 24h post-lesion (**Fig. S2F-G**). These results suggest a fast and specific proliferative response in the ischemia-induced SVZ.

We next analyzed Thbs4 staining in combination with Nestin, an NSC marker, and Doublecortin (DCX), a marker of neuroblasts, before and after MCAO. SVZ was analyzed in sham and ischemic mice 7-, 15- and 30-days post-ischemia (dpi). The immunofluorescence analysis of the SVZ (**Fig. 2A**) showed a transient decrease in Nestin and DCX-positive cells but an increase of Thbs4-positive astrocytes up to 15 dpi (**Fig. 2B-D**) compared to sham animals. The increase of Thbs4 astrocytes was also confirmed by Western blot analysis using SVZ homogenates (**Fig. 2E-F**), evidencing a 2-fold increased expression of Thbs4 in the ischemic SVZ. Similarly to immunofluorescence, Western blot also showed decreased Nestin protein levels at 15 dpi (**Fig. 2G**). These results demonstrate that Thbs4 expression in the SVZ increases after ischemia, coinciding with a decrease in neuroblast markers, suggesting that the classical pro-neuroblast program of the SVZ is interrupted in favor of the generation of astrocytes after ischemia.

Characterization of ischemia-induced cell populations in the SVZ

To characterize the different cell populations of the SVZ activated after focal ischemia, we labeled the whole pool of proliferating cells with 1% BrdU in drinking water for 14 days before MCAO (Codega et al., 2014). One month after MCAO, BrdU in the SVZ primarily stained slow proliferative cells like type B cells, whereas in rapid transit-amplifying cells (type C), BrdU was diluted away. Therefore, we chose to label type C cells by intraperitoneal administration (50 mg/kg) of 5-Iodo-2'-deoxyuridine (IdU) 24h before euthanasia (**Fig. 3A**). To identify the cellular origin of newborn astrocytes, we analyzed the SVZ 30 dpi by immunofluorescence co-labeling Thbs4 and GFAP together with BrdU or IdU. We found a 2-fold increase in the total amount of proliferative cells (BrdU-positive) after MCAO with respect to the sham group (**Fig. 3B**), whereas we did not observe a significant change in the number of IdU-positive cells (**Fig. 3C**). The number of slow proliferative NSC (Thbs4/GFAP/BrdU) increased linearly after MCAO (**Fig. 3D, E**) especially in the dorsal region of the SVZ (**Fig. S3A**), whereas the number of activated NSC (Thbs4/GFAP/IdU) did not change significantly, either in the whole SVZ (**Fig. 3F**) or in any subregion analyzed (**Fig. S3B**). These results suggest that, after ischemia, Thbs4-positive astrocytes derive from the slow proliferative type B cells.

Ischemia-induced newborn astrocytes migrate from the dorsal SVZ to ischemic regions

To confirm that Thbs4-positive astrocytes originate from type B cells of dorsal SVZ, we labeled NSCs of dorsal SVZ by electroporating the pCAGGSx-CRE plasmid in P1 Ai14 Rosa26-CAG-tdTomato transgenic mice (**Fig. 4A**). Plasmid electroporation induced the expression of tdTomato (tdTOM) by Cre recombination, enabling the spatial tracking and cell fate assessment of electroporated NCSs from the dorsal SVZ. Three to four months after electroporation, we performed the MCAO, and tdTOM fluorescence was analyzed at 7, 30, and 60 dpi. To confirm the efficient labeling of NSCs by the electroporation protocol, we followed the tdTOM fluorescence in the OB (**Fig. S4A**, see methods). Only those animals with tdTOM-positive cells in the OB were taken into account for later analysis. After quantification of tdTOM-positive NSCs 7, 30, and 60 dpi, we observed a significant decrease in tdTOM-positive cells in ischemic animals in all SVZ regions analyzed (**Fig. 4B-C** and **Fig S4B**), suggesting that they either left the area, or died. Conversely, there was a general increase of tdTOM-positive cells outside the SVZ (**Fig. 4D-E**), especially in the intermediate and caudal axis of the whole brain compared to sham animals (**Fig. S4D-G**), suggesting that electroporated cells had migrated away from the SVZ.

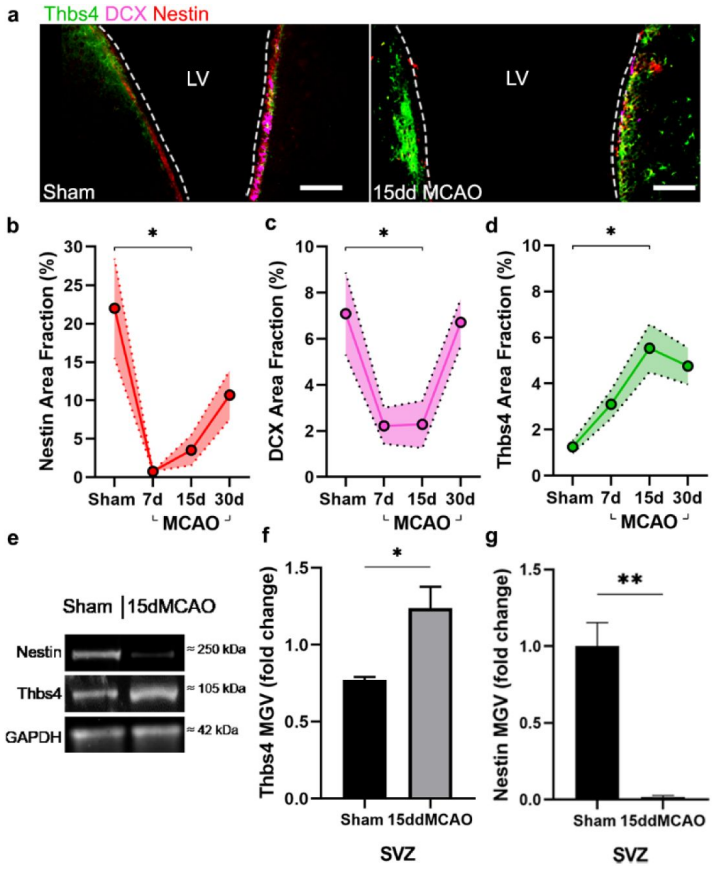

Figure 2

Thbs4 expression is upregulated in the SVZ after brain ischemia.

(a) Representative images of Thbs4 (green), Nestin (red) and DCX (magenta) in the SVZ under physiological conditions (left) and 15 days post-injury (dpi) (right). (b, c) The number of actively proliferating NSCs and neuroblast decreases at 7 and 15 dpi in the SVZ, as shown by reduced Nestin (b) and DCX (c) levels, respectively. (d) Thbs4 expression increases in the SVZ over time following ischemic injury. (e) Representative western blot images of Nestin and Thbs4 in sham and 15 dpi SVZ. (f, g) Quantification of mean gray value (MGV) from (e), normalized to GAPDH, shows an increased in Thbs4 (f) and a decrease in Nestin (g) in the 15 dpi SVZ. Scale bar = 100 μm in (a). n = 6 (b, c, d) and 3 (e, f, g) per condition. Bars represent mean ± SEM. *$p < 0.05$ and **$p < 0.01$; two-tail Student's t test (sham vs. 15ddMCAO) and Tukey post-hoc test (after one-way ANOVA was significant at $p < 0.05$). See also Supplementary Figures 1 and 2.

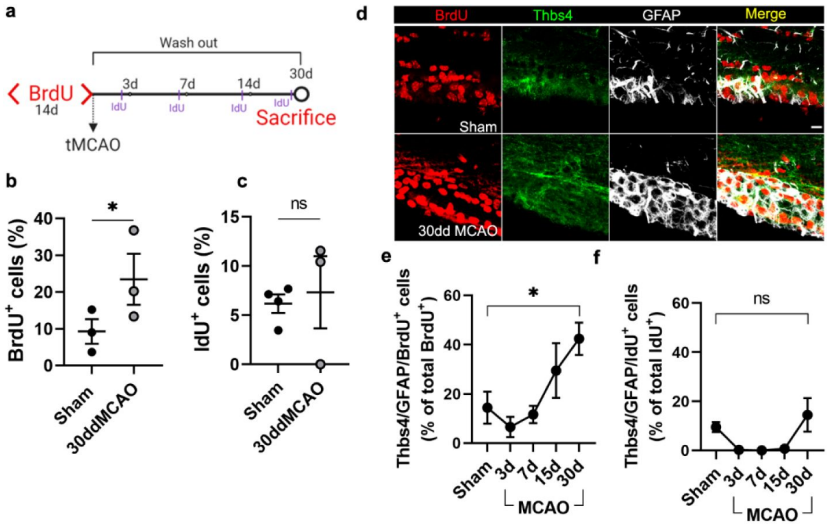

Figure 3

Thbs4-positive cells derive from B-type NSCs in the SVZ after brain ischemia.

(a) Experimental design: chronic BrdU (1% in water) treatment was administered for two weeks. BrdU labeling persisted only in B-type NSCs 30 days after treatment. Animals were injected with IdU (50 mg/kg) three times the day before euthanasia to label proliferating cells. (b, c) BrdU (b) and IdU (c) positive cells in the SVZ. Only BrdU-positive cells showed a significant increase at 30 dpi. (d) Representative confocal images showing Thbs4, GFAP and BrdU levels in sham (top) and 30 dpi mice (bottom). (e, f) Thbs4/GFAP/BrdU positive cells (slow proliferative cells) increased in the SVZ at 30 dpi (e), while no changes were observed in Thbs4/GFAP/IdU positive cells (fast proliferative cells). Scale bar = 10 μm (d). n = 4 (sham) and 3 (MCAO). Bars represent mean ± SEM. *$p < 0.05$ by two-tail Student's t-test (sham vs. 30dd MCAO). See also Supplementary Figure 3.

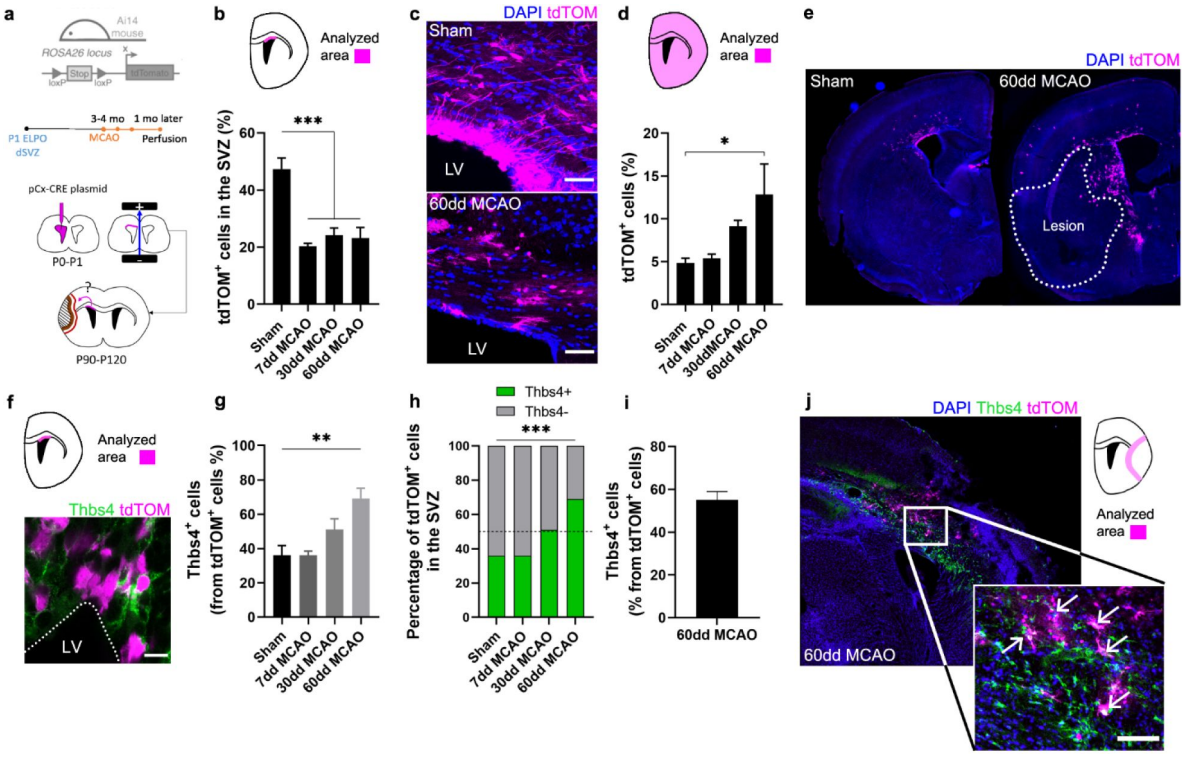

Figure 4

Ischemia-induced Thbs4 astrocytes migrate from the SVZ to ischemic areas.

(a) Experimental design: Ai14, ROSA26-CAG-tdTomato transgenic mice were electroporated in the dorsal SVZ at P1. The pCAGGSx-CRE plasmid induced tdTomato (tdTOM) expression in dorsal NSCs. MCAO was performed 3-4 months later in the same electroporated hemisphere. Mice were analyzed at 7, 30, and 60 dpi. (b) Quantification of tdTOM-positive cells shows a decrease in the dorsal SVZ following brain ischemia. (c) Representative images of tdTOM-positive cells in sham (top) and 60 dpi SVZ (bottom). (d) Quantification of tdTOM-positive cells in the whole brain shows a gradual increase outside the SVZ after brain ischemia. (e) Representative images of tdTOM expression in sham (left) and 60 dpi mice (right). (f) Representative image of Thbs4/tdTOM-positive cells in the dorsal SVZ. (g) Quantification shows an increase in Thbs4/tdTOM-positive cells in the SVZ at 30 and 60 dpi. (h) The proportion of Thbs4-positive cells within the tdTOM-positive pool increases in the SVZ at 30 and 60 dpi. (i) Around 50% of tdTOM-positive cells expressed Thbs4 in the infarcted tissue at 60 dpi. (j) Representative image of Thbs4 and tdTOM expression near the damaged area. Scale bar = 50 μm (c), 10 μm (f), and 100 μm (g). n = 6 animals per condition. Bars represent mean ± SEM. *$p < 0.05$, **$p < 0.01$, and ***$p < 0.001$ by Chi-square test (h) and Tukey post-hoc test (after one-way ANOVA was significant at $p < 0.05$). See also Supplementary Figure 4.

To identify the proportion of NSCs that differentiated into Thbs4-positive astrocytes following ischemia, we analyzed the co-expression of Thbs4 with tdTOM after MCAO. Despite the general decrease of tdTOM-positive cells in the SVZ, the fraction of Thbs4/tdTOM cells increased at 30 dpi after MCAO (**Fig. 4F-G**), reaching a maximum increase at 60 dpi (**Fig. 4H**), in particular in rostral and intermediate SVZ (**Fig. S4C**). Finally, we analyzed the Thbs4-positive astrocytes recruitment to the ischemic regions. More than half of the total tdTOM-positive cells in the infarcted area expressed the Thbs4 marker at 60 dpi (**Fig. 4I-J**). These results suggest that ischemia-induced astrogliogenesis in the SVZ occurs in type B cells from the dorsal region and that these newborn Thbs4-positive astrocytes migrate to the ischemic areas.

Thbs4-positive astrocytes accumulate at the glial scar after brain ischemia

Besides its role in the neurogenic niches, Nestin is also rapidly and locally expressed by reactive astrocytes and participates in glial scar formation (Frisén et al., 1995). Thus, we used Nestin immunofluorescence as a reliable tool to identify the lesion border where the glial scar occurs (**Fig. 5A**). Nestin staining of the scar was also compared with more classical methodologies like TTC staining (**Fig. 5B**), where viable tissue is stained red and dead tissue is left unstained. The white-pale pink area was then measured as infarct tissue by TTC staining (**Fig. 5C**). Unlike the TTC staining, which can only be performed shortly after the lesion, the visualization of the glial scar with Nestin immunofluorescence allowed us to analyze the lesion at later time-points. We observed a rapid formation of the glial scar as early as 7 dpi (**Fig. 5D**). Analyzing the expression of the two astrocytic markers, Thbs4 and GFAP, as a percentage of the glial scar region-of-interest (ROI), we observed different dynamics and localization. GFAP expression increased rapidly after 7 days within the glial scar ROI, whereas Thbs4 was upregulated at 15 dpi (**Fig. 5E**). This delay suggested that the glial scar harbors two different astrocytic sub-populations: GFAP-only or GFAP/Thbs4. To analyze the spatial location of GFAP and Thbs4 markers within the Nestin border, we measured the fluorescence intensity profile of damaged area at 30 dpi. GFAP was found in both the scar and core areas, whereas Thbs4 fluorescence was found mostly at the borders of the glial scar (**Fig. 5F-G**). Analysis and dynamics of Thbs4-positive astrocyte migration were further performed in the corpus callosum (CC), striatum (Str), cortex (Ctx) and olfactory bulb (OB) (**Fig. S5A**). We observed a linear increase of Thbs4-positive astrocytes from 7 to 60 dpi, both in the Ctx and Str (**Fig. S5B**). Migration occurred mainly through the corpus callosum; among the total GFAP-positive astrocytes, 36.5% were also positive for Thbs4, suggesting that more than one-third of the astrocytes in the glial scar originated from the SVZ (**Fig. S5C**). Likewise, the number of DCX-positive cells dramatically decreased 15 dpi in all OB layer (**Fig. S5D-F**) together with a significant decrease of BrdU-positive cells (**Fig. S5G**) DCX/BrdU-positive neuroblasts in the RMS (**Fig. S5H**), suggesting that ischemia induced a change in the neuroblasts' ectopic migratory pathway, depriving the OB layers of SVZ newborn neurons.

Thbs4-positive astrocytes modulate extracellular matrix homeostasis at the glial scar

To investigate the role of Thbs4-positive astrocytes in the glial scar, we analyzed hyaluronic acid (HA), the main component of the brain extracellular matrix (ECM), using the hyaluronic acid binding protein (HABP) as a marker. Following ischemic damage, local astrocytes (GFAP+/Thbs4-) react by adopting a fibrotic morphology, producing high-molecular weight HA (HMW-HA) to form the glial scar and isolate the damaged area (Preston and Sherman, 2011). We then examined HA deposition in the corpus callosum and the infarcted areas after MCAO. HABP immunofluorescence (**Fig. 6A**) and image analysis revealed HA accumulation in the infarcted areas. Skeleton analysis, which quantifies the length of HA chains and correlates with its molecular weight, identified progressively longer HA cable-like structures at the glial scar as the infarct evolved (**Fig. 6B**). Fractal dimension analysis, which reflects the interconnectivity of the extracellular matrix (Soria

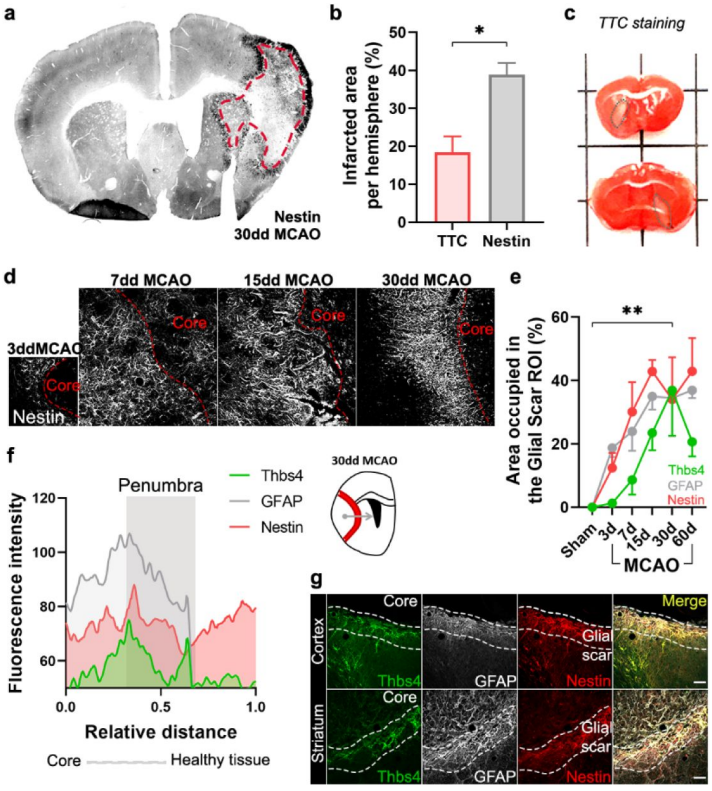

Figure 5

Ischemia-induced Thbs4 astrocytes accumulate at the glial scar.

(a) The glial scar could be observed at 30 dpi using Nestin immunofluorescence. (b) Classical TTC technique underestimated ischemic regions compared with Nestin immunofluorescence. (c) Representative images of TTC staining in infarcted brains. (d) Representative confocal images showing the time course of Nestin expression at 3, 7, 15 and 30 dpi. (e) The Nestin-positive glial scar was established by 15 dpi, while Thbs4 astrocytes arrived at the glial scar later, by 30 dpi. (f) Fluorescence profile of Thbs4, GFAP and Nestin marker from the core to penumbra areas shown Thbs4 was mainly located at the borders of the Nestin-positive glial scar. (g) Representative images of Thbs4 (green), GFAP (white) and Nestin (red) markers in sham (top) and 30 dpi mice (bottom). Scale bar = 50 μm (g). n = 3 animals per condition. Bars/lines represent mean ± SEM. *$p < 0.05$ and **$p < 0.01$ by two-tail Student's t test (TTC vs. Nestin) and by Dunnett posthoc test (after two-way ANOVA was significant at $p < 0.05$). See also Supplementary Figure 5.

et al., 2020), further confirmed HA accumulation and increased matrix complexity in infarcted areas, but not in corpus callosum (**Fig. 6C**), suggesting that ECM accumulation is different in white and gray matter.

The proximity of Thbs4-positive astrocytes to HA in the ischemic scar (**Fig. 6D-E**) led us to investigate if this population contributed to ECM production and, consequently, to scar formation. Since HA is produced exclusively at the cell membrane (Sherman et al., 2015; Zimmermann and Dours-Zimmermann, 2008), we analyzed HA labeling within 1 µm of the Thbs4-positive cell membrane in high-resolution confocal images (**Fig. 6F**). Image analysis showed a significant increase in HABP area at Thbs4-positive astrocyte-cell membranes after MCAO (**Fig. 6G**), suggesting a role of Thbs4-positive astrocytes in HA production within the glial scar.

To explore the potential role of Thbs4-positive astrocytes in HA removal, we quantified intracellular HABP spots in Thbs4-positive astrocytes at the glial scar. While HMW-HA cleavage occurs extracellularly, HA fragments can be internalized for degradation by lysosomal hyaluronidases (Preston and Sherman, 2011; Zimmermann and Dours-Zimmermann, 2008). Intracellular HABP spots were compared between Thbs4-positive astrocytes and local astrocytes (GFAP-positive/Thbs4-negative) (**Fig. S6A**). Thirty days after MCAO, Thbs4-positive astrocytes showed more intracellular HABP than local astrocytes in the infarcted cortex (**Fig. S6B**). However, the number of HA spots internalized was higher in local astrocytes compared with Thbs4 astrocytes (**Fig. S6C**), suggesting that Thbs4-positive cells internalize HA in fewer vesicles. To confirm that astrocytes were degrading HA, we performed an immunofluorescence analysis of CD44 (**Fig. S6D**). CD44 is a transmembrane glycoprotein receptor that mediates HA internalization and degradation, and therefore ECM remodeling (Dzwonek and Wilczynski, 2015). We detected that around 50% of the total Thbs4-positive astrocytes contained internalized CD44 receptor, in the striatum 30 dpi (**Fig. S6E**), with higher numbers (60%) for the infarcted corpus callosum. These findings suggest that Thbs4-positive astrocytes participate in both the formation and degradation of the extracellular matrix at the glial scar.

To further investigate HA internalization by astrocytes, we conducted *in vitro* experiments using rat SVZ neural stem cells cultures. An oxygen and glucose deprivation (OGD) protocol was applied as an ischemia model and cells were fixed 7 days after OGD (**Fig. S7A**). HA was analyzed via HABP immunofluorescence (**Fig. S7B**), both inside and outside the Thbs4-positive cells (**Fig. S7C**). Thbs4-positive cells showed increased intracellular HA after OGD (**Fig. S7D**), while extracellular HA levels decreased (**Fig. S7E**). However, this phenomenon was reversed after adding hyaluronidases in the extracellular space (**Fig. S7F-G**), suggesting that Thbs4-positive cells from SVZ homogenates can internalize or synthesize HA depending on external stimuli. HA internalization was also measured in Iba1-positive cell cultures where we observed a reduced internalization compare to Thbs4-positive cells (**Fig. S7H**). Lastly, metalloproteinase activity was found to be increased in Thbs4 cultures following OGD (**Fig. S7I**). Altogether, these results suggest Thbs4-positive cells can internalize HA after ischemic conditions but also synthetize it when ECM is degraded.

Hyaluronan accumulation is sufficient but not exclusive for the recruitment of Thbs4-positive astrocytes

Since Thbs4-positive astrocytes migrate to the glial scar but not to the ischemic core, we hypothesized that HA, the primary component of the ischemic scar, may be the trigger signal for recruiting Thbs4-positive astrocytes. To test this hypothesis, we simulated the ECM accumulation that occurs at the scar by overexpressing the Hyaluronan synthase 2 (HAS2) from the naked mole rat (*Heterocephalus glaber*), a tool often used in mice to produces HA of very high molecular weight (Tian et al., 2013; Zhang et al., 2023). We used a viral vector (AAV2/9-CAG-HAS2-3xFlag) with a FLAG tag to visualize transduced cells after intracerebral inoculation in the striatum and checked HA accumulation in FLAG-positive areas using HABP staining (**Fig. 7A**). We

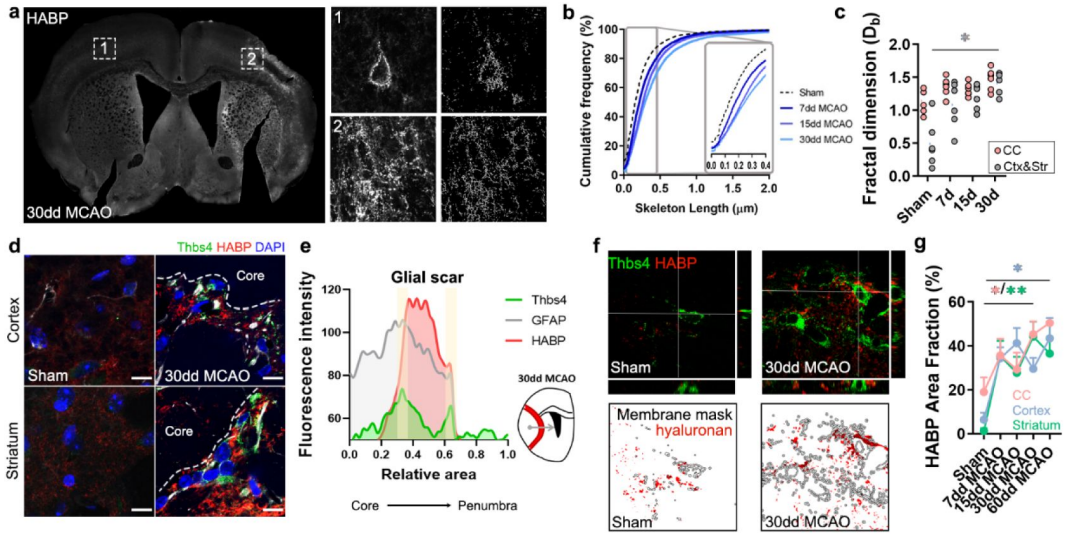

Figure 6

Thbs4-positive astrocytes produce hyaluronan at the glial scar after MCAO.

(a) Representative images of hyaluronic acid (HA) labeled with HABP in the contralateral (1) and ipsilateral hemisphere (2). Only perineuronal nets are clearly visible in the healthy tissue, while a dense interstitial matrix is observed in ischemic areas. (b) Cumulative distribution of skeletonized HA signal in sham and infarcted regions of 7, 15 and 30 dpi mice ($p < 0.0001$). (c) Quantification of fractal dimension showed increased extracellular matrix interconnectivity in the infarcted cortex and striatum (Ctx & Str) at 30 dpi. (d) Representative confocal images of Thbs4 (green) and HABP (red) in the cortex and striatum of sham and 30 dpi mice. Note the HA labelling on the surface of Thbs4-positive cells. (e) Fluorescence intensity profile of Thbs4, GFAP and HABP markers from the lesion core to penumbra areas. Thbs4 expression was mainly restricted to the borders of the HA-positive glial scar at 30 dpi. (f) Representative confocal images of Thbs4 and HABP markers in sham and 30 dpi mice (top). Examples of HA (red) occupying the membrane mask of Thbs4-positive astrocytes in sham and 30 dpi mice (bottom), showing increased HA synthesis after MCAO. (g) Quantification of membrane-bound HA showed increased HA along Thbs4-positive membrane after brain ischemia (corpus callosum: pink; infarcted cortex: blue; infarcted striatum: green). Scale bar = 10 µm (e). n = 6 animals per condition. *$p < 0.05$ and ****$p < 0.0001$ by Krustal Wallis test and two-way ANOVA (significant at $p < 0.05$). See also Supplementary Figures 6 and 7.

overexpressed HAS2 (or GFP as control) unilaterally. In a subset of animals that underwent MCAO, AAV-HAS2 was injected contralateral to the infarct, to compare Thbs4-positive astrocytes recruitment by both stimuli, the inflammation from the ischemic damage and the HA accumulation *per se* (**Fig. 7B**). FLAG-positive cells were quantified as a surrogate marker of viral infection for both control and MCAO groups (**Fig. 7C**). The GFP control group did not increase HA production *per se* (**Fig. 7D**). However, HA overexpression was observed in HAS2 groups (both control and MCAO group) by HABP immunofluorescence (**Fig. 7E-F**).

HA accumulation was sufficient to recruit the Thbs4-positive astrocytes from the ipsilateral SVZ 45 days after AAV-HAS2 inoculation (**Fig. 7G**), with a similar time window to that observed after MCAO. Interestingly, when we induced a lesion by MCAO and performed viral overexpression of HAS2 in the contralateral hemisphere, we found that Thbs4-positive astrocytes preferentially migrated to the ischemic glial scar (**Fig. 7G**). This migration of Thbs4-positive astrocytes to the site of ischemic damage occurred despite no differences in HA overexpression between contralateral (HAS2 infected) and ipsilateral (infarcted area) hemispheres (**Fig. 7H**). These results suggest that the accumulation of HMW-HA alone is sufficient to activate and recruit Thbs4-positive astrocytes from the SVZ. However, the preferential migration to the ischemic scar indicates that brain ischemia generates a more potent biochemical signal that not only activates the SVZ but also recruits newborn astrocytes.

Ischemia-induced gliogenesis at the SVZ correlates with local hyaluronan degradation

It is known that the niche microenvironment has a unique ECM composition (Kjell et al., 2020) and that the stiffness of the niche plays a crucial role in the proliferation and differentiation of progenitor cells (Long and Huttner, 2019; Segel et al., 2019). After observing the close association between Thbs4-positive astrocytes and the ECM at the glial scar, we decided to study the Thbs4/HA tandem in the SVZ following MCAO (**Fig. 8A**). We did not observe any significant changes in the HA area across the entire SVZ but noted a decrease at 7 and 15 dpi in the dorsal SVZ (**Fig. 8B-D**). Skeleton analysis showed fragmentation of HA exclusively in the dorsal SVZ at 7 and 15 dpi (**Fig. 8E-G**), i.e., earlier than the migration of these newborn astrocytes toward the lesion.

Next, we examined the expression of genes related to HA degradation (*Hyase 1*, *2* and *3*) and synthesis (*HAS 1* and *HAS 2*). We also analyzed *Thbs4* and hypoxia-inducible factor 1-alpha (*Hif1a*), which are known to be upregulated in the SVZ following brain ischemia (Benito-Muñoz et al., 2016; Liu et al., 2007). Fresh SVZ tissue was collected from sham, 15 and 30 dpi mice (**Fig. 8H**). We observed an increased expression of all Hyases at 15 dpi and slightly decreased by 30 dpi, whereas synthases (HAS) showed a gradual increase from 15 to 30 dpi (**Fig. 8I**). Additionally, we observed an upregulation of Thbs4 and Hif1a both at 15 and 30 dpi (**Fig. 8I**). These results suggest that HA degradation in the SVZ is correlated with the Thbs4 response to ischemia.

Discussion

The effects of brain insult on adult neurogenesis have been extensively discussed, both in animal models and humans. However, whether these injuries can trigger the generation of newborn astrocytes from the neurogenic niches remains a topic of debate. Neural stem cells in the adult brain are a remnant of embryonic radial glia. Some researchers suggest that depletion of neurogenesis in the adult brain is a consequence of astrogliogenesis (Encinas et al., 2011), while others propose astrogliogenesis is part of a neurorestorative program originating from the neurogenic niches (Bonzano et al., 2018; Sohn et al., 2015). Despite these differing perspectives, direct and definitive evidence of the generation of newborn astrocytes from the SVZ or the SGZ has yet to be presented, as well as the potential role of these astrocytes in aging and

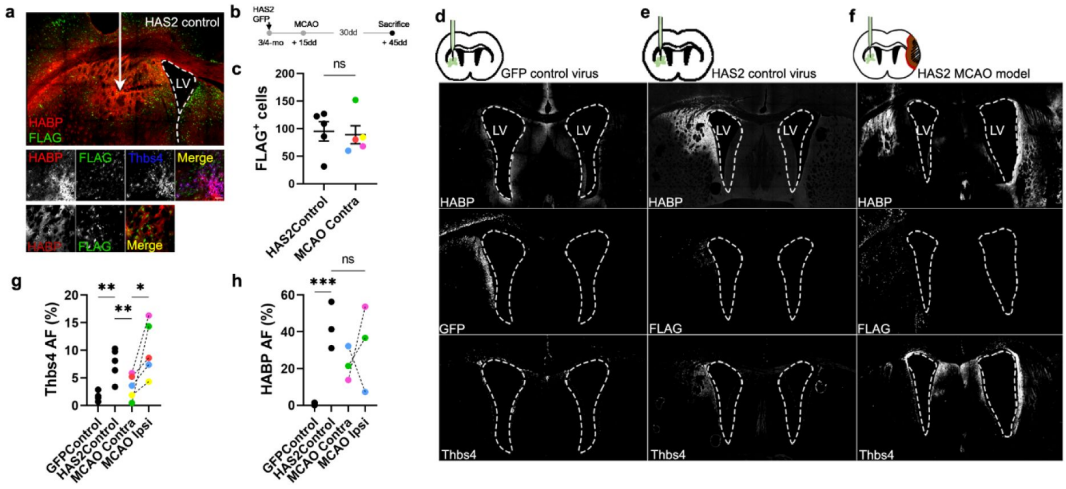

Figure 7

Hyaluronan accumulation is sufficient but not exclusive to recruit Thbs4 astrocytes.

(a) Representative images of HA accumulation caused by viral-mediated overexpression of HAS2 from naked mole rat. (b) Experimental design: HAS2 viral injections were performed 2 weeks before MCAO. Animals were sacrificed 30 days after MCAO. We used standard GFP virus as control. Two groups of HAS2-injected mice were studied, with only one subjected to MCAO. (c) FLAG-positive cells (HAS2 virus tag) did not show changes in either HAS2 control (HAS2Control) or HAS2-MCAO group (contralateral hemisphere). (d, e, f) Representative images of HABP, GFP and Thbs4 markers in GFP control virus (d), HAS2 control virus (e) and HAS2 MCAO group (f). (g) Thbs4 expression increased after HAS2 viral-mediated overexpression. However, Thbs4 was upregulated in the ischemic hemisphere when MCAO was performed together with the HAS2 viral infection (MCAO ipsi). GFP control virus did not induce increase of Thbs4. (h) HABP was used as a control for HA accumulation. Thbs4 astrocytes in HAS2 MCAO group increased in the ischemic hemisphere even though HA accumulation in both hemispheres (HAS2 and MCAO hemisphere), suggesting additional ischemia-induced signals recruit Thbs4 astrocytes to infarcted areas. Scale bar = 100 μm (a). n = 6 animals per condition. *$p < 0.05$, **$p < 0.01$ and ***$p < 0.001$ by two-tail Student's t-test (HAS2Control vs. MCAO Contra) and Tukey posthoc test (after one-way ANOVA was significant at $p < 0.05$).

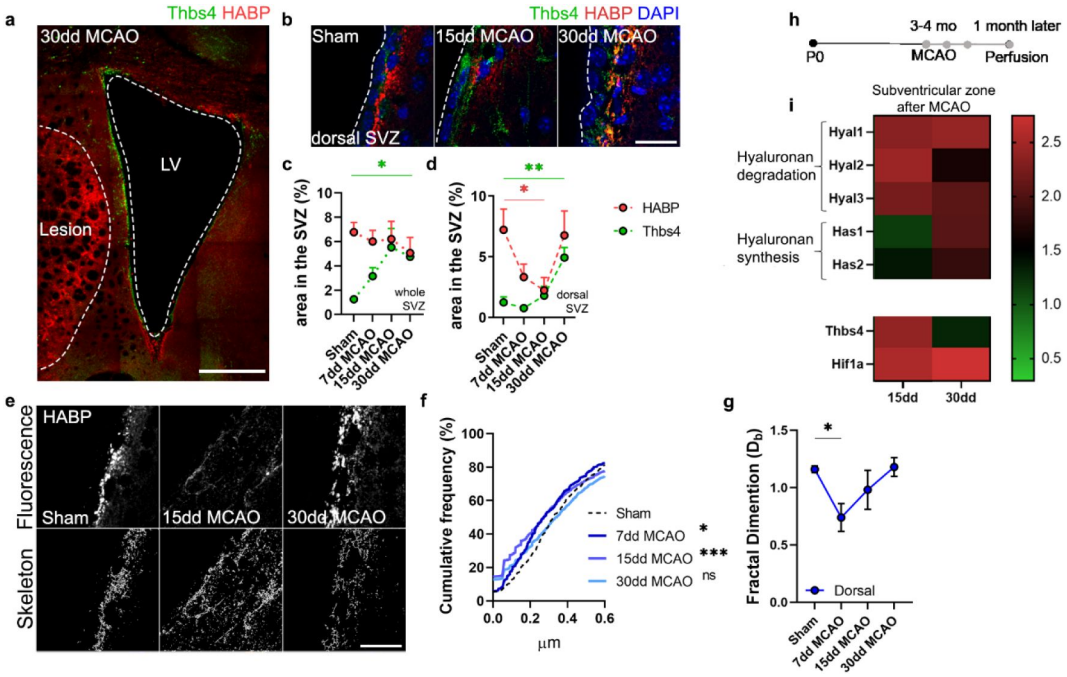

Figure 8

HA degradation in the SVZ correlates with Thbs4 response to brain ischemia.

(a) Representative image of Thbs4 and HA (HABP) markers in the SVZ at 30 dpi. (b) Representative images of Thbs4 and HA in the sham and 15, 30 dpi SVZ. (c, d) HA levels did not change in the entire SVZ after MCAO (c) but decreased significantly in the dorsal SVZ (d). Thbs4 expression increased throughout the SVZ after MCAO (c), with a marked rise at 30 dpi in the dorsal SVZ (d), coinciding with HABP reduction. (e) Representative confocal (top) and skeletonized (bottom) images of HABP in the dorsal SVZ of sham, 15 and 30 dpi mice. (f) Cumulative distribution of HA skeletons showed a reduction in the length of HA cable-like structures only in the dorsal SVZ at 7 and 15 dpi. (g) The interconnectivity of the extracellular matrix decreased by 7 dpi in the dorsal SVZ, as measured by fractal dimension. (h) Experimental design for qPCR: 3–4-month-old mice were subjected to MCAO, and fresh SVZ tissue was extracted 15 and 30 days after MCAO for RT-qPCR analysis. (i) Hyaluronan degradation genes (Hyal1, Hyal2 and Hyal3) increased by 15 and 30 dpi in the SVZ, while hyaluronan synthase genes (HAS1 and HAS2) were overexpressed later, at 30 dpi. Thbs4 and Hif1a were also upregulated by 15 and 30 dpi in the SVZ. Scale bar = 100 µm (a). n = 6 (c, d, e and g) and 3 (i). *$p < 0.05$, **$p < 0.01$ and ***$p < 0.001$ by Krustal Wallis test and Tukey post-hoc test (after one-way ANOVA was significant at $p < 0.05$).

pathological conditions. In this study, we confirm that a strong and acute damage-associated stimulus in the brain, such as an ischemic infarct, prompts astrogliogenesis in the SVZ. Furthermore, we demonstrate that these astrocytes, which are positive for Thbs4, migrate to the glial scar and play a role in its modulation, being capable of synthesis and degradation of hyaluronan, a key component of the ECM at the scar.

Our findings align with previous studies, where cortical injury initiated by photothrombotic/ischemia was shown to trigger a substantial production of Thbs4-positive astrocytes from the SVZ, a process modulated by Notch activation (Benner et al., 2013). In this work, the authors suggested a clear role for Thbs4-positive astrocytes in modulating the ischemic scar. In fact, homozygotic deletion of the Thbs4 gene led to abnormal glial scar formation and increased microvascular hemorrhage following brain ischemia. Similarly, our results demonstrate that the adult neurogenic niche at the SVZ responds early after ischemic stroke, degrading local hyaluronan plausibly to modify niche stiffness and facilitate proliferation and differentiation of NSCs. Further experiments using Thbs4-knockout models will help confirm this hypothesis.

By labeling NSC via *in vivo* postnatal electroporation, we provided proof of the origin and migration of newborn Thbs4-positive astrocytes from the SVZ to the ischemic scar in response to the injury. Notably, Thbs4 is expressed in the newborn astrocytes that migrate to the scar, whereas local reactive astrocytes at the site of injury express only GFAP. It is likely that SVZ-derived newborn astrocytes require Thbs4 expression to facilitate their migration to the ischemic area, as Thbs4 deletion has been shown to impair migration of SVZ-derived cells along the RMS (Girard et al., 2014).

It is noteworthy that while the local, “GFAP-only”, reactive astrocytes at the scar are capable of forming the required ECM (Cregg et al., 2014; Wanner et al., 2013), we show that Thbs4-positive (Thbs4/GFAP) astrocytes are also recruited from the SVZ to modulate scar formation. Unlike local reactive astrocytes, which are hastily generated and present both at the core and periphery of the lesion, the newborn astrocytes from the SVZ arrive later to the injury. We demonstrate that these Thbs4-positive astrocytes migrate from the SVZ to the lesion and halt at the lesion border (precisely defined by Nestin staining), establishing residence at the scar but not beyond.

The molecular signals that trigger gliogenesis in the SVZ and recruit newborn astrocytes to the lesion remain unclear. We previously identified adenosine, a byproduct of ATP hydrolysis, as a strong candidate, as it stimulates astrogliogenesis through A1 receptors following OGD *in vitro* and ischemia *in vivo* (Benito-Muñoz et al., 2016). Here, we show that viral-mediated overproduction of HA, the primary component of the glial scar, is sufficient to activate the generation and migration of the Thbs4-positive astrocytes from the SVZ. However, our findings also show that the ischemic infarct, with its proinflammatory (cytokines, chemokines) and proteolytic (MMPs, ROS) signals (Jayaraj et al., 2019), serves as a more potent attractor than the ECM alone.

The glial response from the SVZ we propose in this study can have several functional implications. Thbs4-positive astrocytes generated from the SVZ might act as a second wave of reactivity, supporting local astrocytes in modulating ECM formation. Hyper-reactive astrocytes at the lesion border decrease over time, along with reductions in HA synthesis and CD44 activity, suggesting that the second wave of Thbs4-positive astrocytes from the SVZ could sustain high levels of HA production (Lindwall et al., 2013). Thus, Thbs4-positive astrocytes may be crucial during this delayed temporal window when glial scar remodeling is essential for neurological recovery (Cai et al., 2017; Dzyubenko et al., 2018). However, it’s important to note that only about one-third of the astrocytes at the glial scar are derived from the SVZ. This suggests that while SVZ-derived astrocytes may be important for glial scar maintenance, local astrocytes remain the central players in this process.

Based on our observations of both HA production and internalization by Thbs4-positive astrocytes *in vivo* within the ischemic region and *in vitro* following OGD, we propose a role for these astrocytes in the modulation, and possibly maintenance, of the ECM at the scar. It is likely that ECM degradation at the scar is also carried out by professional macrophages, such as microglia, which are known to be recruited to the scar (Fawcett and Asher, 1999) and have been shown to degrade ECM through phagocytosis (Nguyen et al., 2020; Soria et al., 2020). Understanding which cells within the scar environment participate in its modulation, particularly its degradation, holds highly therapeutic value for promoting regeneration (Dzyubenko et al., 2018; Silver and Miller, 2004). Here, we shed light on the unknown role of SVZ-derived astrocytes activated by ischemic brain injury and propose them as critical players in tissue regeneration after brain ischemia.

Acknowledgements

The authors thank Juan Carlos Chara, Zara Martínez-Paez, and Laura Escobar for their invaluable technical support. We thank Laura Simon for proofreading the manuscript, and Abraham Martín, Mónica Benito-Muñoz and Sol Beccari for training in MCAO in mice. We also thank Vera Gorbunova (University of Rochester, USA) for providing the cDNA of HAS2 from the naked mole rat. We thank Marie-Laure Thiolat and Dr. Nathalie Dutheil for AAV production. This study received financial support from the French government in the framework of the University of Bordeaux's IdEx "Investments for the Future" program/GPR BRAIN_2030 (B.D.). F.C. acknowledges funding from BIOEF (BIO21/COV/012), Eukampus, Plan Complementario en Salud (PRTR-C17.I1) and the Basque Government. F.N.S. was funded by the Spanish Research Agency (IJCI-2017-32114, PID2020-115896RJ-I00 and RYC2021-032602-I co-funded by NextGeneration EU/PRTR). C.M. acknowledges funding from the Basque Government (IT1203-19) and CIBERNED. M.A. was supported by a PhD fellowship from the Basque Government.

Author contributions

M.A. conducted experiments and collected and analyzed data. M.C.T. and H.C. provided the Ai14-Rosa26-CAG-tdTomato$^{flx/flx}$ mice and technical input for electroporation. B.D. provided the AAV-HAS2 and conceived the idea of glial scar simulation. F.C., F.N.S. and C.M. secured funding. C.M. provided infrastructural support and scientific feedback. F.C. and F.N.S. conceived and supervised the study. F.P.C. supervised the study. M.A. and F.N.S. prepared the figures. M.A., F.N.S. and F.C. wrote the paper, with input from all authors.

Methods

Animals

Male and female wild-type C57BL6/J mice and Ai14-Rosa26-CAG-tdTomato$^{flx/flx}$ transgenic mice bred at the animal facility of UPV/EHU were used for *in vivo* experiments. Sprague Dawley rat pups from P4 to P7 were used for *in vitro* experiments. All animals for *in vitro* and *in vivo* studies were handled in accordance with the European Communities Council Directive (2010/63/EU). All possible efforts were made to minimize animal suffering and the number of animals used. Animals were maintained under standard laboratory conditions with food and water *ad libitum*.

Transient MCAO

Brain ischemia was induced in 3-4-month old C57BL/6 mice (approximately 25 g) by occluding 60 minutes of the lenticulo-striate arteries with a 10 mm length of silicone-coated 6-0 monofilament nylon suture (602223PK10, Doccol Corporation) using a modification of the protocol described by (Gelderblom et al., 2009). Arteries occlusion generated a specific lesion in the cortex and striatum that was evaluated at different times after the MCAO (7, 15, 30 or 60 days after occlusion). Ischemic damage was evaluated in the ipsilateral hemisphere by Cresyl violet staining, Nestin immunofluorescence or hyaluronan staining. Sham animals, in which arteries were visualized but not disturbed, were used as an experimental control. Both experimental groups, sham and ischemic, were anesthetized with a mix of isoflurane and oxygen (induction of anesthesia with 4% isoflurane and maintenance for surgery at 1.5% isoflurane) and maintained under analgesia with buprenorphine 24 hours after ischemia (0.03 mg/Kg body weight i.p. every 12h). Animal wellness was evaluated daily, controlling the body weight and the motor deficit of the animal by means of neurological scores and pole test. Motor deficit was assessed in each animal 1h after MCAO and later every 24h. Animals without neurological deficits were excluded from the study.

5-bromo-2’-deoxyuridine (BrdU) protocol

The total pool of proliferating cells was labelled with three injections of 50 mg/kg 5-bromo-2’-deoxyuridine (BrdU) the day before MCAO protocol. Animals were sacrificed the day after MCAO to analyse acute SVZ proliferation. Chronic BrdU protocol was performed for quiescent NSC identification (Codega et al., 2014). Briefly, 1% of BrdU was administered in the drinking water for 14 days. On day 15, BrdU was removed and animals were subjected to MCAO protocol. Mice were sacrificed and perfused at 3, 7, 15, and 30 days after MCAO, although only animals with a temporal window of 30 days between MCAO and perfusion were used for statistical analysis. Activated cells were labelled by i.p. injection of 50 mg/Kg 5-iodo-2'-deoxyuridine (IdU) 24 hours before euthanasia.

Electroporation

Ai14-Rosa26-CAG-tdTomato$^{flx/flx}$ transgenic mice and pCAGGS-CRE plasmid were kindly provided for Prof. Harold Cremer and Marie-Catherine Tiveron from Institut de Biologie du Développement de Marseille (IBDM). Postnatal electroporation was performed as described previously (Platel et al., 2019). Mice pups from P0-P2 were anesthetized by hypothermia. pCAGGS-CRE plasmid was used at a final concentration of 2.5 µg/ul and 2µl was injected in the lateral ventricle by expiratory pressure using a glass micropipette. Following injection, pup brains were placed between electrodes targeted the dorsal SVZ and subjected to five 95V electrical pulses (50 ms, 950 ms intervals). BTX ECM399 (Thermo Fisher Scientific) electroporator was used with 7 mm tweezer electrodes. Electroporated pups were reanimated at 37°C before returning to the mother.

In order to analyze the Thbs4 positive cells in the SVZ, we subcloned the eGFP gene (from a pCMV-eGFP N1) into a PGL3-basic backbone containing mouse Thbs4 promoter, kindly provided by Stenina-Adognravi lab (Muppala et al., 2017). pThbs4-GFP was also electroporated in P0-P2 mice, and euthanized 1-day post-electroporation to corroborate Thbs4 expression in the SVZ at postnatal stages.

AAV vector production

AAV2/9-CAG-HAS2-3xFlag vector was produced by polyethylenimine (PEI) mediated triple transfection of low passage HEK-293 T/17 cells (ATCC; cat number CRL-11268). The respective AAV expression plasmid expression plasmid pNMRHAS2_N1 (provided by Dr Vera Gorbunova) was cotransfected with the adeno helper pAd Delta F6 plasmid (Penn Vector Core, cat # PL-F-PVADF6) and AAV Rep Cap pAAV2/9 plasmid (Penn Vector Core, cat # PL-TPV008). AAV vector was purified as previously described (Bourdenx et al., 2015). Cells are harvested 72 h post-transfection,

resuspended in lysis buffer (150 mM NaCl, 50 mM Tris–HCl pH 8.5) and lysed by 3 freeze-thaw cycles (37°C/-80°C). The cell lysate is treated with 150 units/ml Benzonase (Sigma, St Louis, MO) for 1 h at 37°C, and the crude lysate is clarified by centrifugation. Vectors are purified by iodixanol step gradient centrifugation and concentrated and buffer-exchanged into Lactated Ringer's solution (Baxter, Deerfield, IL) using vivaspin20 100 kDa cut-off concentrator (Sartorius Stedim, Goettingen, Germany). Titrations were performed at the transcriptome core facility (Neurocentre Magendie, INSERM U862, Bordeaux, France). The genome-containing particle (gcp) titer was determined at a concentration of 1.10^{13} gcp/ml by quantitative real-time PCR using the Light Cycler 480 SYBR green master mix (Roche, cat # 04887352001) with primers specific for the AAV2 ITRs (fwd 50-GGAACCCCTAGTGATG GAGTT-3'; rev 50-CGGCCTCAGTGAGCGA-30) on a Light Cycler 480 instrument. The purity assessment of vector stocks was estimated by loading 10 µl of vector stock on 10 % SDS acrylamide gels; total proteins were visualized using the Krypton Infrared Protein Stain according to the manufacturer's instructions (Life Technologies).

In vivo AAV-HAS2 injections

Mice were anesthetized with isoflurane and fixed to a stereotaxic frame connected with a gas mask. We injected 1µl of adeno-associated virus (AAV2/9) CAG-HAS2-3xFlag (1×10^13 gc/µl) in the contralateral striatum (AP: +1.0; ML: −1.8; DV: −3.2) to simulate scar tissue hyaluronan. After two weeks, the ischemic group was subjected to the MCAO model in the ipsilateral hemisphere and perfused 30 days later. Only slices with representative lesions in both hemispheres were used for image and statistical analysis.

Immunofluorescence

Mice were anesthetized with an intraperitoneal injection of pentobarbital (100 mg/kg). Brain tissues were fixed by intracardiac perfusion using 4% paraformaldehyde. Fixed brains were sliced at 40 µm of thickness using the Leica VT1200S vibratome (Leica Microsystems) and subjected to immunofluorescence. For standard immunofluorescence protocol, tissue slices were permeabilized with 0.1% Triton and non-specific epitopes blocked with 1% Bovine Serum Albumin and 10% Donkey serum in PBS. Primary antibodies (Supplementary Table 1) were incubated at different concentrations (see **Table 1** for specification) overnight at 4°C and then washed three times with 0.1% Triton in PBS. Secondary conjugated antibodies were incubated for 1 h at room temperature. After three washes with 0.1% Triton in PBS, cells were stained for 10 min with DAPI and further washed with PBS. Finally, coverslips were mounted with Fluoromount (SouthernBiotech) and analyzed by fluorescence using the confocal microscope Leica TCS SP8. For hyaluronic acid labeling, endogenous biotins were pre-blocked using Streptavidin/Biotin blocking solution (Vector Labs, #SP-2002) following the manufacturer's instructions and further blocked with PBS 1X 0.1% Saponin 1% BSA for one hour at room temperature. Primary antibodies and biotinylated Hyaluronic Acid Binding Protein (HABP, #385911 Millipore) were incubated for 72 hours at 4°C or 24 hours at room temperature. After three washes with PBS, 1X 0.1% Saponin, secondary antibody and DAPI diluted in the same blocking buffer were incubated for one hour at room temperature. Slices were mounted with Mowiol (Millipore #475904) in superfrost slides (Thermo Fisher Scientific) and #1.5 coverslips.

Imaging and image analysis

Confocal images were acquired in a Leica TCS SP8 with 20x (0.8 NA) and 63x objectives (1.4 NA). Images were taken with a pixel size of 90 nm. Widefield imaging was performed in a Zeiss AxioVision fluorescence microscope and a 3DHISTECH panoramic MIDI II digital slide scanner. Settings were adjusted for each individual experiment and kept for all conditions. Image processing was performed using FIJI (Schindelin et al., 2012), CaseViewer and Hyugens (SVI, The Netherlands) software. For Thbs4, Nestin and DCX immunofluorescence, wholemount SVZ preparations and AAV-HAS2 analysis, tile-scan was done using the navigator plug-in in the LasX software. For Nestin immunofluorescence, images were deconvoluted using the Hyugens software.

Table 1.

Primary antibodies used for in vivo immunofluorescence protocol

Antibody	Host	Isotope	Dilution	Reference	Company
Thbs4	Mouse	Monoclonal IgM kappa light chain	1/400	Sc-390734	Santa Cruz Biotechnology, USA.
Thbs4	Goat	Polyclonal IgG	1/200	AF2390	R&B systems, USA
S100β	Rabbit	Polyclonal	1/400	Z0311	Dako, Agilent Technologies, Inc.
S100β	Mouse	Monoclonal IgG2a	1/1000	MA5-12969	Invitrogen, Spain
GFAP	Mouse	Monoclonal IgG1	1/1000	MAB3402	Sigma, Spain
GFAP	Rabbit	Polyclonal	1/4000	Z0334	Dako, Agilent Technologies, Inc.
βIII tubulin	Rabbit	Polyclonal	1/400	ab18207	Abcam, UK
NeuN	Mouse	Monoclonal IgG1	1/1000	MAB377	Millipore, Germany
DCX	Rabbit	Polyclonal IgG	1/500	ab18723	Abcam, UK
Nestin	Chicken	Polyclonal IgY	1/1000	NES	Aves Lab, EEUU
Prominin 1	Rat	Monoclonal IgG1 kappa	1/300	14-1331-82	Invitrogen, Spain
EGFR	Mouse	Monoclonal	1/400	SAB4200809	Abcam, UK
BrdU	Rat	Monoclonal	1/400	MCA2060	Bio-Rad, USA.
BrdU	Mouse	Monoclonal IgG1, kappa	1/500	03-3900	Invitrogen, Spain
IdU	Mouse	Monoclonal IgG2b	1/100	MA5-24879	Invitrogen, Spain
Ki67	Rabbit	Polyclonal IgG	1/400	Ab15580	Abcam, UK
Cleaved-Caspase 3	Rabbit	Monoclonal IgG	1/300	#9664	Cell Signaling, Germany
CD44	Rat	Monoclonal IgG2b	1/500	MA517875	Invitrogen, Spain
FLAG	Mouse	Monoclonal IgG1	1/500	F1804	Sigma, Spain
Olig2	Mouse	Monoclonal IgG2aκ	1/1000	MABN50	Millipore, Germany

Table 2.

Primer sequences for qPCR

Name	Sequence
Hyal1_FW	GTGCCAAGCCCTATGCTAATAAG
Hyal1_REV	GCATGTCCATTGCAAAGACTGA
Hyal2_FW	GTCCCACATACACCCGAGGA
Hyal2_REV	GGCACTCTCACCGATGGTAGA
Hyal3_Ffw	GGACGACCTGATGCAGACTATTG
Hyal3_REV	GGTCCCCCCAGAGTACCACT
Has1_FW	AGGGCTCTTAAAGGAGGAGTCC
Has1_REV	AGAAGGTAAACTGAGTCCCCAGAA
Has2_FW	CAAAGAGGTTCGTTCAAGTTCTGA
Has2_REV	TGTGTTTGTTTCCCACTAGCTCTC
Hif1a_FW	CATAAAGTCTGCAACATGGAAGGT
Hif1a_REV	ATTTGATGGGTGAGGAATGGGTT
HPRT1_FW	TGATAGATCCATTCCTATGACTGTAGA
HPRT1_REV	AAGACATTCTTTCCAGTTAAAGTTGAG

SVZ images were reconstructed using the tile-scan tool (LasX software, Leica). SVZ region of interest (ROI) was delimited manually and expression of each marker was measured in the SVZ ROI. Quantification of all markers was done manually, except for HABP quantification, which was done with custom FIJI scripts for in vitro (*https://github.com/MariArdaya/Hyaluronan_v2*) and in vivo analysis (*https://github.com/SoriaFN/Tools*). The HABP signal was segmented with an automatic threshold and colocalized with other markers such as CD44. This, combined with cell segmentation, based on the Thbs4 mask, allowed for quantification of HABP area and number of spots inside cells, outside cells or at the membrane (with a band ROI of 1 µm). The Analyze Skeleton and Fractal count plugins were used on the skeletonized segmented HABP to quantify the longest shortest path and the fractal dimension, respectively, to reveal the length and interconnectivity of the matrix network (Casey et al., 2024; Soria et al., 2020).

Western blot

The SVZ was freshly dissected on ice and minced using a micro grinder. Total protein was extracted after tissue lysis with RIPA buffer (Thermo Fisher Scientific #89900) and Protease and Phosphatase Inhibitor Cocktail 100X (Thermo Fisher Scientific). Samples were lysed in ice for 10 minutes and sonicated using an Ultrasonic Processor (Hielscher Ultrasound Technology). Sonicated tissues were centrifuged at 1200 rpm for 10 min and 4°C to remove insoluble fragments. Protein concentration was measured by chemioluminescence using RC DC™ Protein Assay (Bio-Rad). Forty micrograms of protein samples were denatured in reducing loading buffer containing β-mercaptoethanol (M3148, Sigma) and 0.0002% bromophenol blue at 95°C for 5 minutes and separated in pre-casted 12% or 7.5% Tris-Glycine polyacrylamide gel using the Criterion cell system (Biorad). Electrophoresis was conducted at 80 V in a Tris-Glycine buffer (25 mM Tris, 192 mM glycine, 0.1% SDS in dH2O, pH 8.3). After complete separation, proteins were transferred to a nitrocellulose membrane (Biorad) using Trans-Blot® TurboTM Transfer System (Bio-Rad). Nitrocellulose membranes were incubated in blocking solution (Tris-Buffer Solution (TBS), 0.1% Tween-20 and 5% BSA) for one hour at room temperature. Primary antibodies were incubated overnight at 4°C. Horseradish peroxidase-conjugated secondary antibodies were incubated in blocking buffer for one hour at room temperature. Immunodetection was performed by electrochemical luminescence in a Chemidoc MP (Biorad) and the intensity of the bands was quantified using ImageLab (Bio-Rad) software corrected by Gaussian curves.

qRT-PCR

Fresh SVZ tissue from ipsilateral hemisphere was isolated as previously described from sham, 15 and 30 days after MCAO animals to analyze the expression of several genes (Supplementary Table 2). After mechanical trituration, RNA was extracted from the tissue after mechanical trituration following the manufactureŕs protocol (NZYTECH Total RNA Isolation kit protocol (NZYTECH, MB13402). RNA concentration was measured by spectrophotometry using the Nanodrop 2000c spectrophotometer (Thermo-Scientific, USA). Real time polymerase chain reaction (RT-PCR) from 10 ng of RNA was performed using the One-step NZYTECH RT-qPCR Green kit according to manufactureŕs protocol (NZYTECH, MB34302). RT-PCR was normalized using the housekeeping genes hypoxanthine phosphoribosyl-transferase 1 (HPRT1, Qiagen QuantiTect Primer Assay, Barcelona, Spain). Specificity of each amplification was confirmed by melting curve analysis. PCR reactions were performed in a CFX96 Detection System (BioRad, Madrid, Spain). Semi-quantification was performed using the 2-ΔΔCt algorithm. Unsupervised hierarchical distance matrix and distance matrix map was developed using Orange3 software (Python v3.0).

Statistical analysis

Statistical analysis was done using GraphPad Prism software (version 8.0; GraphPad software). Data are presented as mean ± SEM unless specified otherwise. Statistical analysis was performed using unpaired Student's t-test for independent conditions and paired Student's t-test for dependent conditions. In addition, one-way and two-way ANOVA were also performed to compare

more than 2 groups among them. Tukey and Dunnett post-hoc tests were used. For HABP skeleton analysis, Kruskal-Wallis analysis was performed to compare cumulative frequency curves in more than 2 groups. *P* value was considered significant at $p < 0.05$. Sample number (*n*), *p* values and statistical test are indicated in figure legends.

Supplementary information

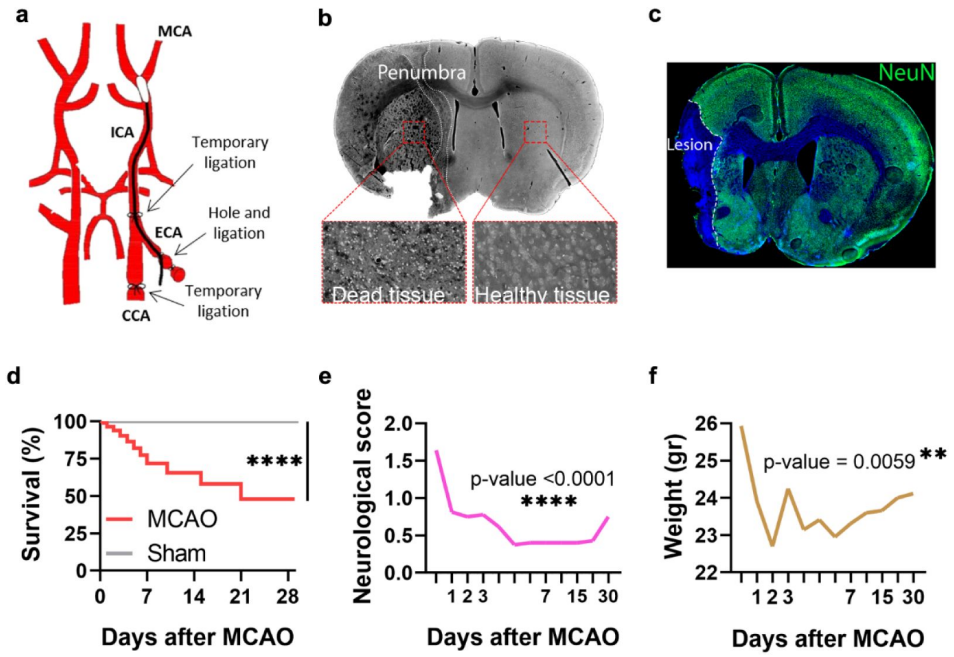

Supplementary Figure 1

Characterization of the Middle Cerebral Artery Occlusion (MCAO) mouse model of brain ischemia.

Related to **Figure 2**. (a) Scheme of the procedure: 10 mm silicon-coated filament was inserted through an external artery and re-directed to the internal one. Ischemia was induced after 60 minutes of occlusion. After that, the filament was removed, and animals were observed every day before euthanasia. (b) Volume of infarction was observed by cresyl violet staining. (c) Neuronal death was observed by NeuN immunofluorescence. (d) Around 50% of ischemic mice survived at 28 dpi. (e) Ischemic animals ameliorated neurological symptoms over time. (f) Weight was measured as controls for mice healthcare. n = 17 (d, e, f). $^{**}p < 0.01$ and $^{****}p < <0.0001$ by survival curve test and Tukey post-hoc test (after one-way ANOVA was significant at $p < 0.05$).

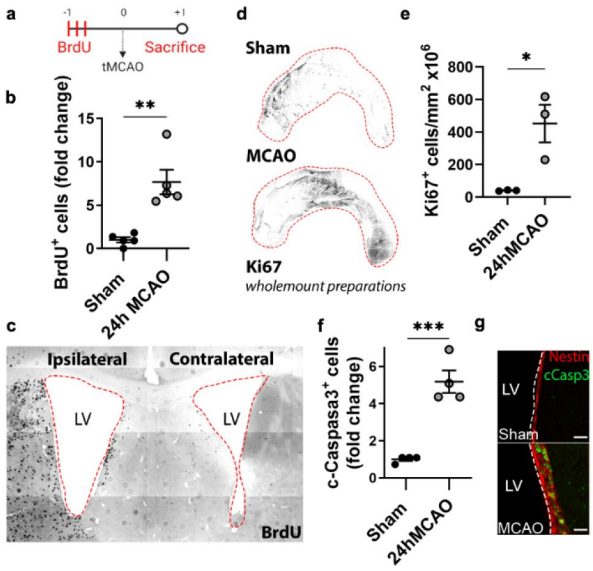

Supplementary Figure 2

Cell proliferation in the SVZ after brain ischemia.

Related to **Figure 2**. (a) Experimental design: three BrdU (50mg/kg) injections were performed the day before MCAO protocol. Animals were sacrificed 24 hours after the brain stroke model. (b) BrdU-positive cells increased in the SVZ 24 hours after MCAO. (c) Representative image of BrdU positive cells in the ipsilateral (left) and contralateral (right) hemisphere 24 hours after MCAO. (d) Ki67 marker was also used to analyze cell proliferation in wholemount preparations of the SVZ. (e) Ki67 positive cells increased in the SVZ 24 hours after MCAO. (f) The Cleaved-Caspase 3 marker increased in the SVZ 24 hours after MCAO. (g) Cleaved-caspase 3 marker was used to assess apoptosis in the SVZ after brain ischemia. Scale bar = 15 μm (g). n = 5 (sham) and 4 (MCAO). Bars represent mean ± SEM. *$p < 0.05$, **$p < 0.01$ and ***$p < 0.001$ by two-tail Student's t-test (sham vs. 24h MCAO).

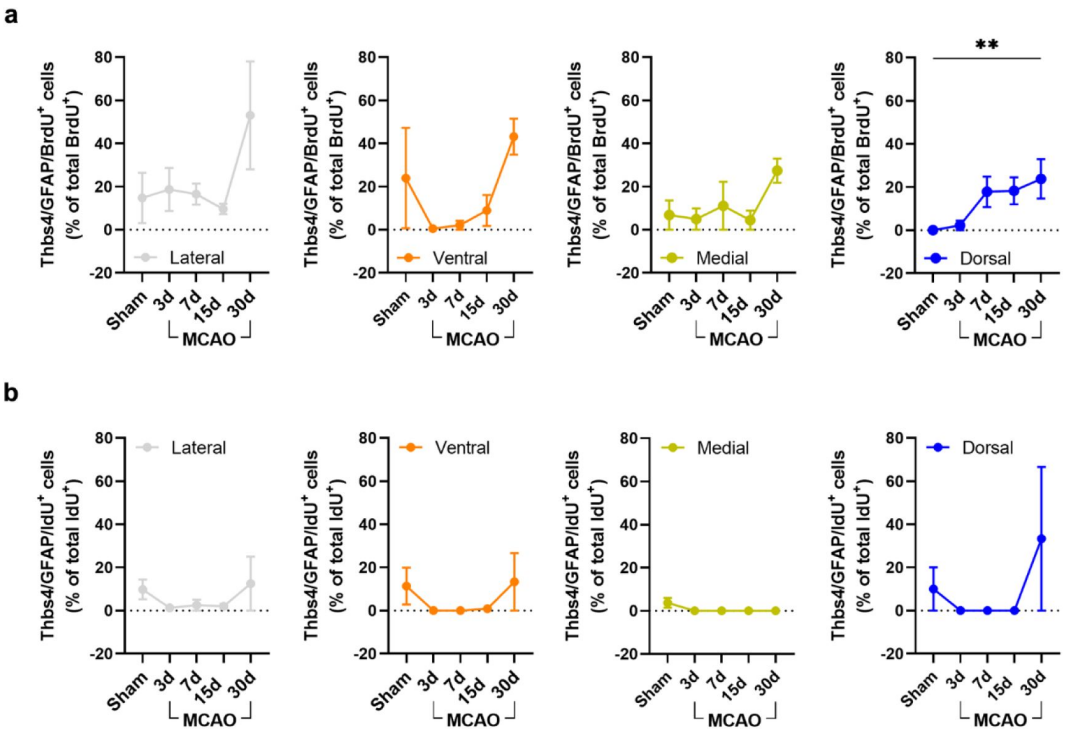

Supplementary Figure 3

Thbs4 astrocytes derive from slow proliferative cells after brain ischemia.

Related to **Figure 3**. (a) Slow proliferative cells were quantified in the lateral (grey), ventral (orange), medial (yellow) and dorsal (blue) SVZ. We only observed an increase of Thbs4/GFAP/BrdU positive cells in the dorsal SVZ 30 dpi. (b) Thbs4/GFAP/IdU positive cells did not show changes in the lateral (grey), ventral (orange), medial (yellow) and dorsal (blue) SVZ after brain ischemia. n = 4 (sham) and 3 (MCAO). $^{**}p < 0.01$ by by two-tail Student's t-test (sham vs. 30dd MCAO).

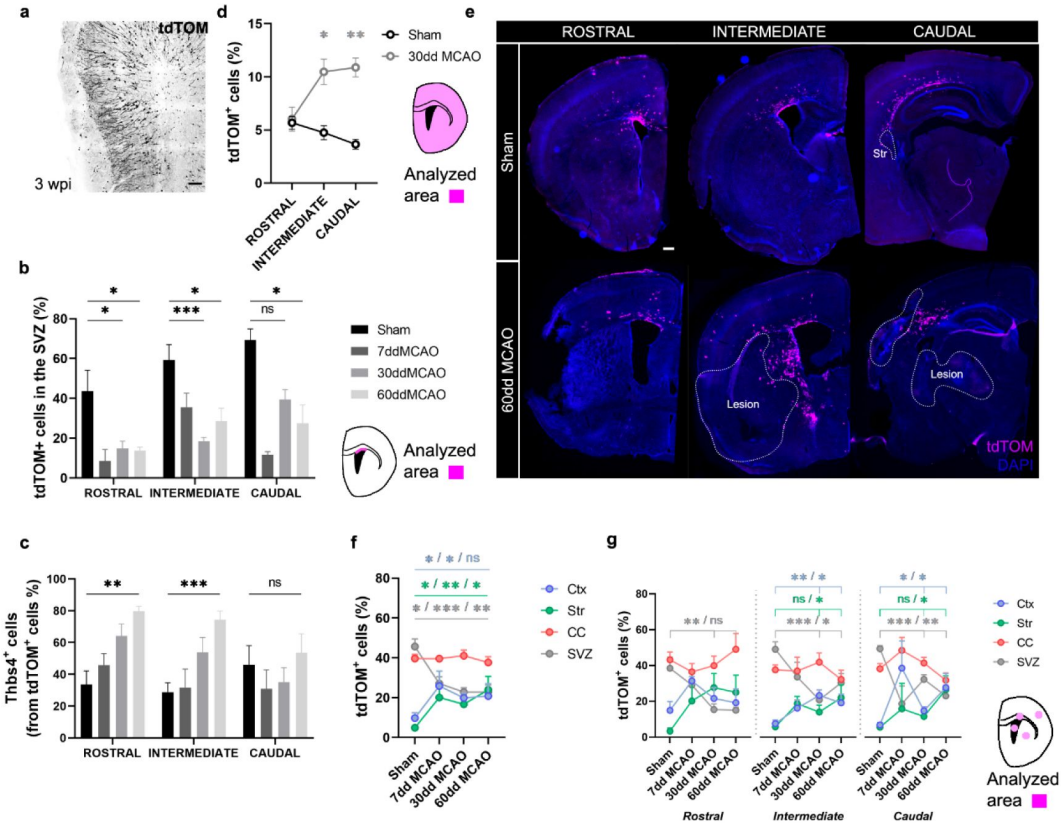

Supplementary Figure 4

Ischemic-induced Thbs4 astrocytes migrate preferentially to caudal infarcted areas.

Related to **Figure 4**. (a) Representative image of tdTOM positive cells in the OB three weeks after electroporation (3wpi). (b) tdTOM-positive cells decreased in the rostral, intermediate and caudal SVZ 7, 30 and 60 dpi. (c) Thbs4/tdTOM positive cells increased in rostral and intermediate SVZ 30 and 60 dpi. (d) Expression of tdTomato increased in intermediate and caudal brain areas at 30 dpi. (e) Representative images of tdTOM expression in rostral (left), intermediate (middle) and caudal (right) brain areas of sham (top) and 60 dpi mice (bottom). (f) tdTOM positive cells increased in the infarcted cortex (Ctx) and striatum (Str) whereas decreased in the dorsal SVZ (SVZ). No changes were observed in the corpus callosum (CC). (g) tdTOM positive cells only increased in the infarcted cortex and striatum at intermediate and caudal brain regions. Scale bar = 100 μm (a) and 1000 μm (e). n = 6 animals per condition. Bars represent mean ± SEM. *$p < 0.05$, **$p < 0.01$ and ***$p < 0.001$ by Dunnett/Tukey post-hoc test (after two-way ANOVA was significant at $p < 0.05$).

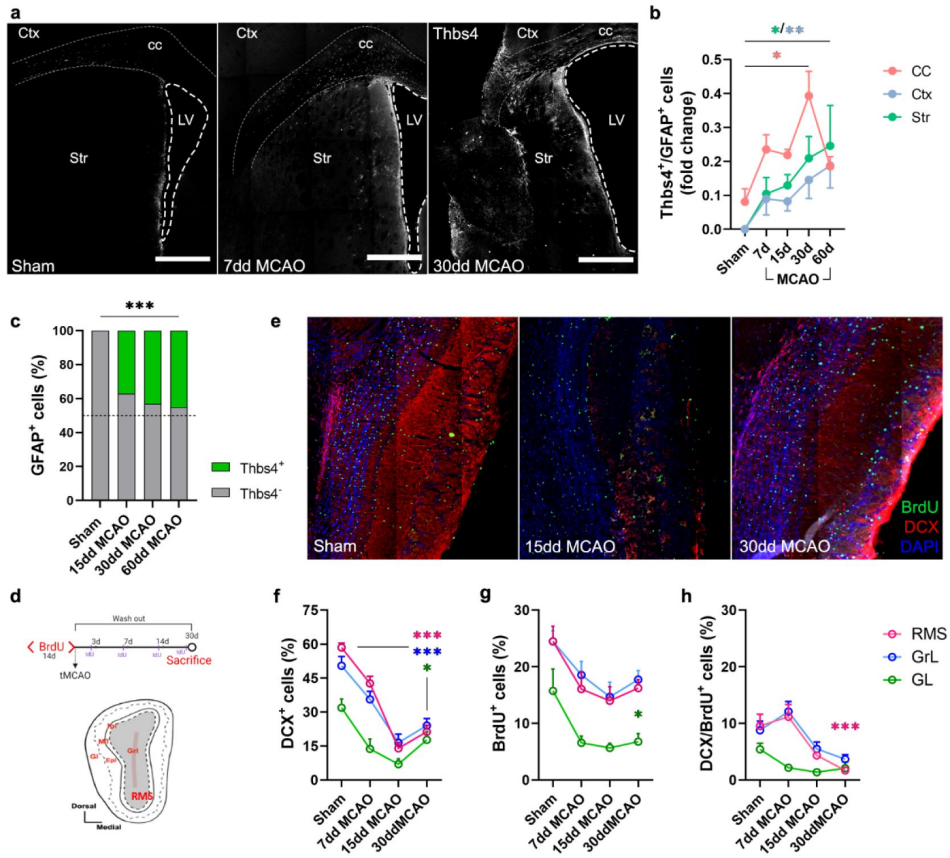

Supplementary Figure 5

SVZ NSC stop producing newborn neurons to send newborn astrocytes to the ischemic areas.

Related to **Figure 5**. (a) Thbs4 expression in the corpus callosum (cc), infarcted cortex (Ctx) and infarcted striatum (Str) of sham and 7 and 30 dpi mice. (b) Thbs4 increased by 30 dpi in the corpus callosum (cc) and 60 dpi in the infarcted cortex (Ctx) and infarcted striatum (Str). (c) Expression of Thbs4 increased in total GFAP population after 15, 30 and 60 dpi. (d) Experimental design: chronic BrdU (1% in water) treatment was administered for two weeks. BrdU only persisted in slow proliferative NSC (Codega et al., 2014). DCX and BrdU positive cells were measured in the OB layers 7, 15 and 30 dpi. (e) Representative images of BrdU and DCX marker in sham (left), 15 (middle) and 30 (right) dpi mice OB. (f) DCX positive cells decreased 15 and 30 dpi in the RMS, granular OB layer (GrL) and glomerular OB layer (GL). (g) BrdU positive cells only decreased 30 dpi in the glomerular OB layer (GL). Double DCX/BrdU positive cells significative decreased in the RMS 30 dpi. In (f) and (g), values are normalized to total DAPI nuclei (100%). Scale bar = 500 μm (a). n = 6 animals per condition. Lines represent mean ± SEM. *$p < 0.05$, **$p < 0.01$ and ***$p < 0.001$ by Chi-square test and Tukey post-hoc test (after two-way ANOVA was significant at $p < 0.05$).

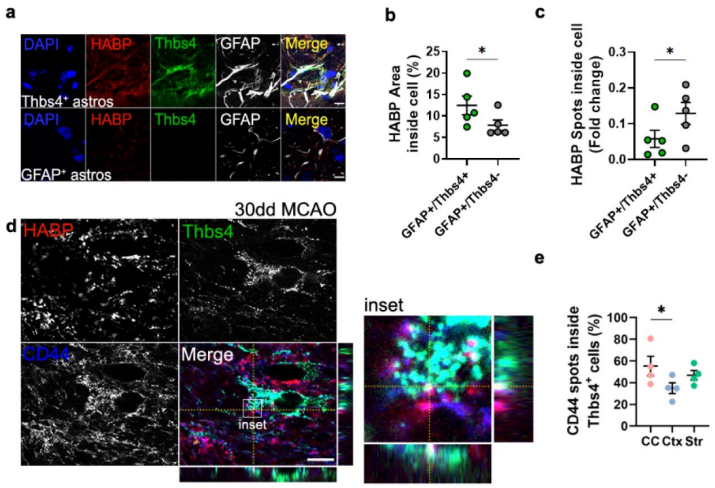

Supplementary Figure 6

Thbs4 astrocytes internalize HA in the infarcted areas.

Related to **Figure 6**. (a) Representative images of Thbs4/GFAP ("newborn astrocytes", top) and GFAP-only ("local astrocytes", bottom) cells in the infarcted areas at 30 dpi. (b) Thbs4-positive astrocytes internalized more HA compared to local astrocytes only labelled with GFAP marker. (c) However, the number of HA spots internalized was higher in local astrocytes compared with Thbs4 astrocytes, suggesting that Thbs4 internalize HA in fewer vesicles. (d) Representative images of HABP (red), Thbs4 (green) and CD44 (blue) at the lesion border. Inset shows an orthogonal projection of Thbs4/CD44/HABP-positive intracellular vesicle. (e) Thbs4 positive astrocytes expressed a high rate of CD44 receptors so much in corpus callosum (CC), infarcted cortex (Ctx) as in infarcted striatum (Str). Scale bar = 10 μm (c, f). n = 5 animals per condition. Bars represent mean ± SEM. *$p < 0.05$ and **$p < 0.01$ by Tukey posthoc test (after two-way ANOVA was significant at $p < 0.05$) and two-tail Student's t-test (Thbs4 vs GFAP).

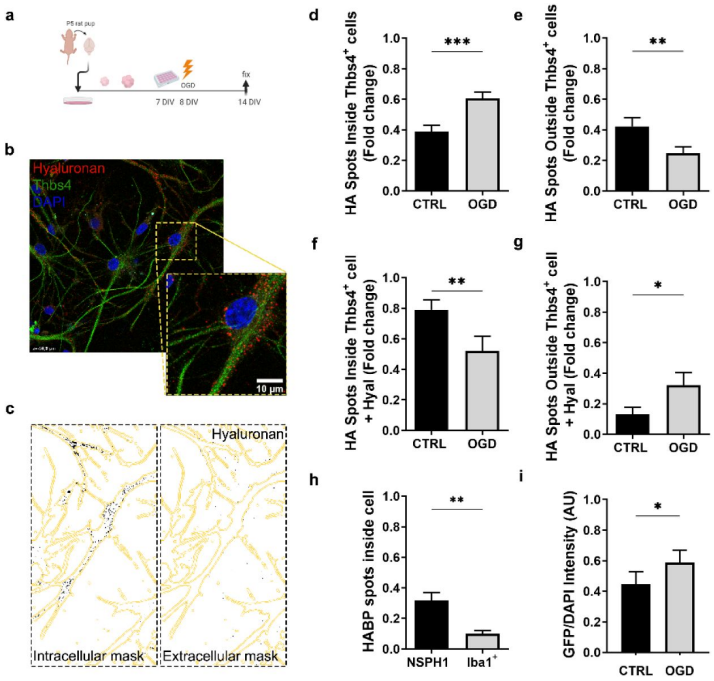

Supplementary Figure 7

In vitro NSC-derived Thbs4 cells synthetize HA after a hypoxic-ischemic condition.

Related to **Figure 6**. (a) Experimental design: P4 pup rats were sacrificed, and SVZ NSC were extracted and cultured in the proliferative medium for one week. After that, neurospheres were disaggregated and seeded isolated in a culture dish. The following day, oxygen and glucose deprivation protocol (OGD) was performed. Cells were fixed 7 days after culture them. (b) Representative images of in vitro Thbs4 positive cells (green) and HA (red). (c) HA spots were measured inside and outside Thbs4 positive cells. (d) HA spots increased inside Thbs4 positive astrocytes after OGD whereas (e) decreased in the extracellular space. However, when NSC were exposed to hyaluronidases in order to remove extracellular HA, Thbs4 positive cells decreased internalization of HA spots (f) and increased extracellular HA spots (g). (h) Neurosphere-derived NSC (NSPH1) internalized more HA spots compared with Iba1-positive cells. (i) Metalloproteinase activity was higher in OGD NSC cultures compared to control condition. Scale bar = 10 µm (b). n = 15 samples per condition. Bars represent mean ± SEM. *$p < 0.05$, **$p < 0.01$ and ***$p < 0.001$ by two-tail Student's t-test (CTRL vs. OGD; NSPH1 vs. Iba1$^+$).

References

Adams KL, Gallo V (2018) **The diversity and disparity of the glial scar** *Nat Neurosci* **21**:9–15 https://doi.org/10.1038/s41593-017-0033-9

Anderson MA, Burda JE, Ren Y, Ao Y, O'Shea TM, Kawaguchi R, Coppola G, Khakh BS, Deming TJ, Sofroniew MV (2016) **Astrocyte scar formation aids central nervous system axon regeneration** *Nature* **532**:195–200 https://doi.org/10.1038/nature17623

Arvidsson A, Collin T, Kirik D, Kokaia Z, Lindvall O (2002) **Neuronal replacement from endogenous precursors in the adult brain after stroke** *Nat Med* **8**:963–970 https://doi.org/10.1038/nm747

Basak O *et al.* (2018) **Troy+ brain stem cells cycle through quiescence and regulate their number by sensing niche occupancy** *Proc Natl Acad Sci U S A* **115**:E610–E619 https://doi.org/10.1073/pnas.1715911114

Beckervordersandforth R *et al.* (2010) **In vivo fate mapping and expression analysis reveals molecular hallmarks of prospectively isolated adult neural stem cells** *Cell Stem Cell* **7**:744–758 https://doi.org/10.1016/j.stem.2010.11.017

Benito-Muñoz M, Matute C, Cavaliere F (2016) **Adenosine A1 receptor inhibits postnatal neurogenesis and sustains astrogliogenesis from the subventricular zone** *Glia* **64**:1465–1478 https://doi.org/10.1002/glia.23010

Benner EJ, Luciano D, Jo R, Abdi K, Paez-Gonzalez P, Sheng H, Warner DS, Liu C, Eroglu C, Kuo CT (2013) **Protective astrogenesis from the SVZ niche after injury is controlled by Notch modulator Thbs4** *Nature* **497**:369–373 https://doi.org/10.1038/nature12069

Bond AM, Ming G-L, Song H (2015) **Adult Mammalian Neural Stem Cells and Neurogenesis: Five Decades Later** *Cell Stem Cell* **17**:385–395 https://doi.org/10.1016/j.stem.2015.09.003

Bonzano S, Crisci I, Podlesny-Drabiniok A, Rolando C, Krezel W, Studer M, De Marchis S. (2018) **Neuron-Astroglia Cell Fate Decision in the Adult Mouse Hippocampal Neurogenic Niche Is Cell-Intrinsically Controlled by COUP-TFI In Vivo** *Cell Rep* **24**:329–341 https://doi.org/10.1016/j.celrep.2018.06.044

Bourdenx M *et al.* (2015) **Lack of additive role of ageing in nigrostriatal neurodegeneration triggered by α-synuclein overexpression** *Acta Neuropathol Commun* **3** https://doi.org/10.1186/s40478-015-0222-2

Bush TG, Puvanachandra N, Horner CH, Polito A, Ostenfeld T, Svendsen CN, Mucke L, Johnson MH, Sofroniew MV (1999) **Leukocyte infiltration, neuronal degeneration, and neurite outgrowth after ablation of scar-forming, reactive astrocytes in adult transgenic mice** *Neuron* **23**:297–308 https://doi.org/10.1016/s0896-6273(00)80781-3

Cai H, Ma Y, Jiang L, Mu Z, Jiang Z, Chen X, Wang Y, Yang G-Y, Zhang Z (2017) **Hypoxia Response Element-Regulated MMP-9 Promotes Neurological Recovery via Glial Scar Degradation and Angiogenesis in Delayed Stroke** *Molecular Therapy* **25**:1448–1459 https://doi.org/10.1016/j.ymthe.2017.03.020

Casey DT, Lahue KG, Mori V, Herrmann J, Hall JK, Suki B, Janssen-Heininger YMW, Bates JHT (2024) **Local fractal dimension of collagen detects increased spatial complexity in fibrosis** *Histochem Cell Biol* **161**:29–42 https://doi.org/10.1007/s00418-023-02248-8

Cavaliere F, Dinkel K, Reymann K (2006) **The subventricular zone releases factors which can be protective in oxygen/glucose deprivation-induced cortical damage: an organotypic study** *Exp Neurol* **201**:66–74 https://doi.org/10.1016/j.expneurol.2006.03.020

Ceanga M, Dahab M, Witte OW, Keiner S (2021) **Adult Neurogenesis and Stroke: A Tale of Two Neurogenic Niches** *Frontiers in Neuroscience* **15**

Cebrian-Silla A *et al.* (2021) **Single-cell analysis of the ventricular-subventricular zone reveals signatures of dorsal and ventral adult neurogenesis** *eLife* **10** https://doi.org/10.7554/eLife.67436

Chaker Z, Codega P, Doetsch F (2016) **A mosaic world: puzzles revealed by adult neural stem cell heterogeneity** *WIREs Developmental Biology* **5**:640–658 https://doi.org/10.1002/wdev.248

Codega P, Silva-Vargas V, Paul A, Maldonado-Soto AR, DeLeo AM, Pastrana E, Doetsch F (2014) **Prospective Identification and Purification of Quiescent Adult Neural Stem Cells from Their In Vivo Niche** *Neuron* **82**:545–559 https://doi.org/10.1016/j.neuron.2014.02.039

Cregg JM, DePaul MA, Filous AR, Lang BT, Tran A, Silver J (2014) **Functional regeneration beyond the glial scar** *Exp Neurol* **253**:197–207 https://doi.org/10.1016/j.expneurol.2013.12.024

Doetsch F, Caillé I, Lim DA, García-Verdugo JM, Alvarez-Buylla A (1999) **Subventricular zone astrocytes are neural stem cells in the adult mammalian brain** *Cell* **97**:703–716 https://doi.org/10.1016/s0092-8674(00)80783-7

Dzwonek J, Wilczynski GM (2015) **CD44: molecular interactions, signaling and functions in the nervous system** *Front Cell Neurosci* **9** https://doi.org/10.3389/fncel.2015.00175

Dzyubenko E, Manrique-Castano D, Kleinschnitz C, Faissner A, Hermann DM (2018) **Role of immune responses for extracellular matrix remodeling in the ischemic brain** *Ther Adv Neurol Disord* **11** https://doi.org/10.1177/1756286418818092

Encinas JM, Michurina TV, Peunova N, Park J-H, Tordo J, Peterson DA, Fishell G, Koulakov A, Enikolopov G (2011) **Division-coupled astrocytic differentiation and age-related depletion of neural stem cells in the adult hippocampus** *Cell Stem Cell* **8**:566–579 https://doi.org/10.1016/j.stem.2011.03.010

Faulkner JR, Herrmann JE, Woo MJ, Tansey KE, Doan NB, Sofroniew MV (2004) **Reactive astrocytes protect tissue and preserve function after spinal cord injury** *J Neurosci* **24**:2143–2155 https://doi.org/10.1523/JNEUROSCI.3547-03.2004

Fawcett JW (2015) **The extracellular matrix in plasticity and regeneration after CNS injury and neurodegenerative disease** *Prog Brain Res* **218**:213–226 https://doi.org/10.1016/bs.pbr.2015.02.001

Fawcett JW, Asher RA (1999) **The glial scar and central nervous system repair** *Brain Res Bull* **49**:377–391 https://doi.org/10.1016/s0361-9230(99)00072-6

Frisén J, Johansson CB, Török C, Risling M, Lendahl U (1995) **Rapid, widespread, and longlasting induction of nestin contributes to the generation of glial scar tissue after CNS injury** *Journal of Cell Biology* **131**:453–464 https://doi.org/10.1083/jcb.131.2.453

Gelderblom M *et al.* (2009) **Temporal and spatial dynamics of cerebral immune cell accumulation in stroke** *Stroke* **40**:1849–1857 https://doi.org/10.1161/STROKEAHA.108.534503

Girard F, Eichenberger S, Celio MR (2014) **Thrombospondin 4 deficiency in mouse impairs neuronal migration in the early postnatal and adult brain** *Molecular and Cellular Neuroscience* **61**:176–186 https://doi.org/10.1016/j.mcn.2014.06.010

Jayaraj RL, Azimullah S, Beiram R, Jalal FY, Rosenberg GA (2019) **Neuroinflammation: friend and foe for ischemic stroke** *J Neuroinflammation* **16** https://doi.org/10.1186/s12974-019-1516-2

Kjell J *et al.* (2020) **Defining the Adult Neural Stem Cell Niche Proteome Identifies Key Regulators of Adult Neurogenesis** *Cell Stem Cell* **26**:277–293

Kralic JE, Ledergerber DA, Fritschy J-M (2005) **Disruption of the neurogenic potential of the dentate gyrus in a mouse model of temporal lobe epilepsy with focal seizures** *European Journal of Neuroscience* **22**:1916–1927 https://doi.org/10.1111/j.1460-9568.2005.04386.x

Lau LW, Cua R, Keough MB, Haylock-Jacobs S, Yong VW (2013) **Pathophysiology of the brain extracellular matrix: a new target for remyelination** *Nat Rev Neurosci* **14**:722–729

Laug D *et al.* (2019) **Nuclear factor I-A regulates diverse reactive astrocyte responses after CNS injury** *J Clin Invest* **129**:4408–4418 https://doi.org/10.1172/JCI127492

Li L, Harms KM, Ventura PB, Lagace DC, Eisch AJ, Cunningham LA (2010) **Focal cerebral ischemia induces a multilineage cytogenic response from adult subventricular zone that is predominantly gliogenic** *Glia* **58**:1610–1619 https://doi.org/10.1002/glia.21033

Lindwall C, Olsson M, Osman AM, Kuhn HG, Curtis MA (2013) **Selective expression of hyaluronan and receptor for hyaluronan mediated motility (Rhamm) in the adult mouse subventricular zone and rostral migratory stream and in ischemic cortex** *Brain Res* **1503**:62–77 https://doi.org/10.1016/j.brainres.2013.01.045

Liu XS, Zhang ZG, Zhang RL, Gregg S, Morris DC, Wang Y, Chopp M (2007) **Stroke induces gene profile changes associated with neurogenesis and angiogenesis in adult subventricular zone progenitor cells** *J Cereb Blood Flow Metab* **27**:564–574 https://doi.org/10.1038/sj.jcbfm.9600371

Llorens-Bobadilla E, Zhao S, Baser A, Saiz-Castro G, Zwadlo K, Martin-Villalba A (2015) **Single-Cell Transcriptomics Reveals a Population of Dormant Neural Stem Cells that Become Activated upon Brain Injury** *Cell Stem Cell* **17**:329–340 https://doi.org/10.1016/j.stem.2015.07.002

Long KR, Huttner WB (2019) **How the extracellular matrix shapes neural development** *Open Biol* **9**

Luskin MB (1993) **Restricted proliferation and migration of postnatally generated neurons derived from the forebrain subventricular zone** *Neuron* **11**:173–189 https://doi.org/10.1016/0896-6273(93)90281-u

Muppala S, Xiao R, Krukovets I, Verbovetsky D, Yendamuri R, Habib N, Raman P, Plow E, Stenina-Adognravi O (2017) **Thrombospondin-4 mediates TGF-β-induced angiogenesis** *Oncogene* **36**:5189–5198 https://doi.org/10.1038/onc.2017.140

Nguyen PT *et al.* (2020) **Microglial Remodeling of the Extracellular Matrix Promotes Synapse Plasticity** *Cell* **182**:388–403

Platel J-C *et al.* (2019) **Neuronal integration in the adult mouse olfactory bulb is a non-selective addition process** *eLife* **8** https://doi.org/10.7554/eLife.44830

Pous L *et al.* (2020) **Fibrinogen induces neural stem cell differentiation into astrocytes in the subventricular zone via BMP signaling** *Nat Commun* **11** https://doi.org/10.1038/s41467-020-14466-y

Preston M, Sherman LS (2011) **Neural Stem Cell Niches: Critical Roles for the Hyaluronan-Based Extracellular Matrix in Neural Stem Cell Proliferation and Differentiation** *Front Biosci (Schol Ed* **3**:1165–1179

Schindelin J *et al.* (2012) **Fiji: an open-source platform for biological-image analysis** *Nat Methods* **9**:676–682

Segel M *et al.* (2019) **Niche stiffness underlies the ageing of central nervous system progenitor cells** *Nature* **573**:130–134

Sherman LS, Matsumoto S, Su W, Srivastava T, Back SA (2015) **Hyaluronan Synthesis, Catabolism, and Signaling in Neurodegenerative Diseases** *International Journal of Cell Biology* **2015**

Silver J, Miller JH (2004) **Regeneration beyond the glial scar** *Nat Rev Neurosci* **5**:146–156 https://doi.org/10.1038/nrn1326

Sohn J, Orosco L, Guo F, Chung S-H, Bannerman P, Mills Ko E, Zarbalis K, Deng W, Pleasure D (2015) **The subventricular zone continues to generate corpus callosum and rostral migratory stream astroglia in normal adult mice** *J Neurosci* **35**:3756–3763 https://doi.org/10.1523/JNEUROSCI.3454-14.2015

Soria FN *et al.* (2020) **Synucleinopathy alters nanoscale organization and diffusion in the brain extracellular space through hyaluronan remodeling** *Nat Commun* **11** https://doi.org/10.1038/s41467-020-17328-9

Sundholm-Peters NL, Yang HKC, Goings GE, Walker AS, Szele FG (2005) **Subventricular Zone Neuroblasts Emigrate Toward Cortical Lesions** *Journal of Neuropathology & Experimental Neurology* **64**:1089–1100 https://doi.org/10.1097/01.jnen.0000190066.13312.8f

Tian X, Azpurua J, Hine C, Vaidya A, Myakishev-Rempel M, Ablaeva J, Mao Z, Nevo E, Gorbunova V, Seluanov A (2013) **High-molecular-mass hyaluronan mediates the cancer resistance of the naked mole rat** *Nature* **499**:346–349

Wanner IB, Anderson MA, Song B, Levine J, Fernandez A, Gray-Thompson Z, Ao Y, Sofroniew MV (2013) **Glial scar borders are formed by newly proliferated, elongated astrocytes that interact to corral inflammatory and fibrotic cells via STAT3-dependent mechanisms after spinal cord injury** *J Neurosci* **33**:12870–12886 https://doi.org/10.1523/JNEUROSCI.2121-13.2013

Yamashita T *et al.* (2006) **Subventricular zone-derived neuroblasts migrate and differentiate into mature neurons in the post-stroke adult striatum** *J Neurosci* **26**:6627–6636 https://doi.org/10.1523/JNEUROSCI.0149-06.2006

Zhang Z *et al.* (2023) **Increased hyaluronan by naked mole-rat Has2 improves healthspan in mice** *Nature* https://doi.org/10.1038/s41586-023-06463-0

Zimmermann DR, Dours-Zimmermann MT (2008) **Extracellular matrix of the central nervous system: from neglect to challenge** *Histochem Cell Biol* **130**:635–653 https://doi.org/10.1007/s00418-008-0485-9

Editors

Reviewing Editor
Annalisa Scimemi
University at Albany, State University of New York, Albany, United States of America

Senior Editor
Sofia Araújo
University of Barcelona, Barcelona, Spain

Reviewer #1 (Public review):

Summary:

The authiors show that SVZ derived astrocytes respond to a middle carotid artery occlusion (MCAO) hypoxia lesion by secreting and modulating hyaluronan at the edge of the lesion (penumbra) and that hyaluronin is a chemoattractant to SVZ astrocytes. They use lineage tracing of SVZ cells to determine their origin. They also find that SVZ derived astrocytes express Thbs-4 but astrocytes at the MCAO-induced scar do not. Also, they demonstrate that decreased HA in the SVZ is correlated with gliogenesis. While much of the paper is descriptive/correlative they do overexpress Hyaluronan synthase 2 via viral vectors and show this is sufficient to recruit astrocytes to the injury. Interestingly, astrocytes preferred to migrate to the MCAO than to the region of overexpressed HAS2.

Strengths:

The field has largely ignored the gliogenic response of the SVZ, especially with regards to astrocytic function. These cells and especially newborn cells may provide support for regeneration. Emigrated cells from the SVZ have been shown to be neuroprotective via creating pro-survival environments, but their expression and deposition of beneficial extracellular matrix molecules is poorly understood. Therefore, this study is timely and important. The paper is very well written and the flow of results logical.

Comments on revised version:

The authors have addressed my points and the paper is much improved. Here are the salient remaining issues that I suggest be addressed.

The authors have still not shown, using loss of function studies, that Hyaluronan is necessary for SVZ astrogenesis and or migration to MCAO lesions.

(1) The co-expression of EGFr with Thbs4 and the literature examination is useful.

(2) Too bad they cannot explain the lack of effect of the MCAO on type C cells. The comparison with kainate-induced epilepsy in the hippocampus may or may not be relevant.

(3) Thanks for including the orthogonal confocal views in Fig S6D.

(4) The statement that "BrdU+/Thbs4+ cells mostly in the dorsal area" and therefore they mostly focused on that region is strange. Figure 8 clearly shows Thbs4 staining all along the striatal SVZ. Do they mean the dorsal segment of the striatal SVZ or the subcallosal SVZ? Fig. 4b and Fig 4f clearly show the "subcallosal" area as the one analysed but other figures show the dorsal striatal region (Fig. 2a). This is important because of the well-known embryological and neurogenic differences between the regions.

(5) It is good to know that the harsh MCAO's had already been excluded.

(6) Sorry for the lack of clarity - in addition to Thbs4, I was referring to mouse versus rat Hyaluronan degradation genes (Hyal1, Hyal2 and Hyal3) and hyaluronan synthase genes (HAS1 and HAS2) in order to address the overall species differences in hyaluronan biology thus justifying the "shift" from mouse to rat. You examine these in the (weirdly positioned) Fig. 8h,i. Please add a few sentences on mouse vs rat Thbs4 and Hyaluronan relevant genes.

(7) Thank you for the better justification of using the naked mole rat HA synthase.

https://doi.org/10.7554/eLife.96076.2.sa2

Reviewer #3 (Public review):

Summary:

The authors aimed to study the activation of gliogenesis and the role of newborn astrocytes in a post-ischemic scenario. Combining immunofluorescence, BrdU-tracing and genetic cellular labelling, they tracked the migration of newborn astrocytes (expressing Thbs4) and found that Thbs4-positive astrocytes modulate the extracellular matrix at the lesion border by synthesis but also degradation of hyaluronan. Their results point to a relevant function of SVZ newborn astrocytes in the modulation of the glial scar after brain ischemia. This work's major strength is the fact that it is tackling the function of SVZ newborn astrocytes, whose role is undisclosed so far.

Strengths:

The article is innovative, of good quality, and clearly written, with properly described Materials and Methods, data analysis and presentation. In general, the methods are designed properly to answer the main question of the authors, being a major strength. Interpretation of the data is also in general well done, with results supporting the main conclusions of this article.

In this revised version, the points raised/weaknesses were clarified and discussed in the article.

https://doi.org/10.7554/eLife.96076.2.sa1

Author response:

The following is the authors' response to the original reviews.

> ***Reviewer #1 (Public Review):***
>
> *The authors show that SVZ-derived astrocytes respond to a middle carotid artery occlusion (MCAO) hypoxia lesion by secreting and modulating hyaluronan at the edge of the lesion (penumbra) and that hyaluronan is a chemoattractant to SVZ astrocytes. They use lineage tracing of SVZ cells to determine their origin. They also find that SVZ-derived astrocytes express Thbs-4 but astrocytes at the MCAO-induced scar do not. Also, they demonstrate that decreased HA in the SVZ is correlated with gliogenesis. While much of the paper is descriptive/correlative they do overexpress Hyaluronan synthase 2 via viral vectors and show this is sufficient to recruit astrocytes to the injury. Interestingly, astrocytes preferred to migrate to the MCAO than to the region of overexpressed HAS2.*
>
> *Strengths:*
>
> *The field has largely ignored the gliogenic response of the SVZ, especially with regard to astrocytic function. These cells and especially newborn cells may provide support for regeneration. Emigrated cells from the SVZ have been shown to be neuroprotective via creating pro-survival environments, but their expression and deposition of beneficial extracellular matrix molecules are poorly understood. Therefore, this study is timely and important. The paper is very well written and the flow of results is logical.*
>
> *Weaknesses:*
>
> *The main problem is that they do not show that Hyaluronan is necessary for SVZ astrogenesis and or migration to MCAO lesions. Such loss of function studies have been carried out by studies they cite (e.g. Girard et al., 2014 and Benner et al., 2013). Similar approaches seem to be necessary in this work.*

We appreciate the comments by the reviewer. The article is, indeed, largely descriptive since we attempt to describe in detail what happens to newborn astrocytes after MCAO. Still, we have not attempted any modification to the model, such as amelioration of ischemic damage. This is a limitation of the study that we do not hide. However, we use several experimental approaches, such as lineage tracing and hyaluronan modification, to strengthen our conclusions.

Regarding the weaknesses found by the reviewer, we do not claim that hyaluronan is necessary for SVZ astrogenesis. Indeed, we observe that when the MCAO stimulus (i.e. inflammation) is present, the HMW-HA (AAV-Has2) stimulus is less powerful (we discuss this in line 330-332). We do claim, and we believe we successfully demonstrate, the reverse situation: that SVZ astrocytes modulate hyaluronan, not at the SVZ but at the site of MCAO, i.e. the scar. However, regarding whether hyaluronan is necessary for SVZ astrogenesis, we only show a correlation between its degradation and the time-course of astrogenesis. We suggest this result as a starting point for a follow-up study. We have included a phrase in the discussion (line 310), stating that further experiments are needed to fully establish a link between hyaluronan and astrogenesis in the SVZ.

> *Major points:*
>
> *(1) How good of a marker for newborn astrocytes is Thbs4? Did you co-label with B cell markers like EGFr? Is the Thbs4 gene expressed in B cells? Do scRNAseq papers show it is expressed in B cells? Are they B1 or B2 cells?*

We chose Thbs4 as a marker of newborn astrocytes based on published research (Beckervordersanforth et al., 2010; Benner et al., 2013; Llorens-Bobadilla et al. 2015, Codega et al, 2014; Basak et al., 2018; Mizrak et al., 2019; Kjell et al., 2020; Cebrian-Silla et al., 2021). From those studies, at least 3 associate Thbs4 to B-type cells based on scRNAseq data (LlorensBobadilla et al. 2015; Cebrian-Silla et al., 2021; Basak et al., 2018). We have included a sentence about this and the associated references, in line 92.

We co-label Thbs4 with EGFR, but in the context of MCAO. We observed an increase of EGFR expression with MCAO, similar to the increase in Thbs4 alongside ischemia (see author). We did not include this figure in the manuscript since we did not have available tissue from all the time points we used (7d, 60d post-ischemia).

Author response image 1.

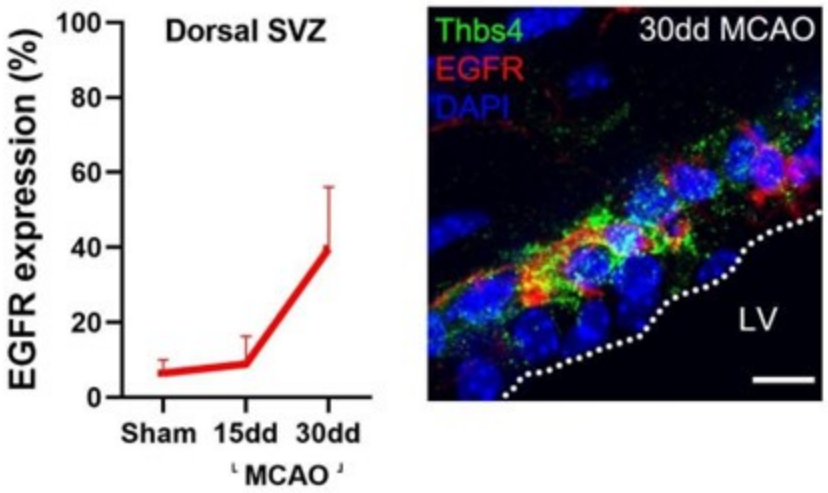

Thbs4 cells, in basal and ischemic conditions, only represent a small amount of IdU-positive cells (Fig 3F), suggesting that they are mostly quiescent cells, i.e., B1 cells. However, the scRNAseq literature is not consistent about this.

> *(2) It is curious that there was no increase in Type C cells after MCAO - do the authors propose a direct NSC-astrocyte differentiation?*

Type C cells are fast-proliferating cells, and our BrdU/IdU experiment (Fig. 3) suggests that Thbs4 cells are slow-proliferating cells. Some authors suggest (Encinas lab, Spain) that when the hippocampus is challenged by a harsh stimulus, such as kainate-induced epilepsy, the NSCs differentiate directly into reactive astrocytes and deplete the DG neurogenic niche (Encinas et al., 2011, Cell Stem Cell; Sierra et al., 2015, Cell Stem Cell). We believe this might be the case in our MCAO model and the SVZ niche, since we observe a decrease in DCX labeling in the olfactory bulb (Fig S5) and an increase in astrocytes in the SVZ, which migrate to the ischemic lesion. We did not want to overcomplicate an already complicated paper, dwelling with direct NSC-astrocyte differentiation or with the reactive status of these newborn astrocytes.

> *(3) The paper would be strengthened with orthogonal views of z projections to show colocalization.*

We thank the reviewer for this observation. We have now included orthogonal projections in the critical colocalization IF of CD44 and hyaluronan (hyaluronan internalization) in Fig S6D, and a zoomed-in inset. Hyaluronan membrane synthesis is already depicted with orthogonal projection in Fig 6F.

> *(4) It is not clear why the dorsal SVZ is analysed and focused on in Figure 4. This region emanates from the developmental pallium (cerebral cortex anlagen). It generates some excitatory neurons early postnatally and is thought to have differential signalling such as Wnt (Raineteau group).*

We decided to analyze in depth the dorsal SVZ after the BrdU experiment (Fig S3), where we observed an increase in BrdU+/Thbs4+ cells mostly in the dorsal area. Hence, the electrodes for electroporation were oriented in such a way as to label the dorsal area. We appreciate the paper by Raineteau lab, but we assume that this region may potentially exploit other roles (apart from excitatory neurons generated early postnatally) depending on the developmental stage (our model is in adults) and/or pathological conditions (MCAO).

> *(5) Several of the images show the lesion and penumbra as being quite close to the SVZ. Did any of the lesions contact the SVZ? If so, I would strongly recommend excluding them from the analysis as such contact is known to hyperactivate the SVZ.*

We thank the referee for the suggestion to exclude the harsher MCAO-lesioned animals from the analysis. Indeed, the MCAO ischemia, methodologically, can generate different tissue damages that cannot be easily controlled. Thus, based on TTC staining, we had already excluded the more severe tissue damage that contacted the SVZ, based on TTC staining.

> *(6) The authors switch to a rat in vitro analysis towards the end of the study. This needs to be better justified. How similar are the molecules involved between mouse and rat?*

We chose the rat culture since it is a culture that we have already established in our lab, and that in our own hands, is much more reproducible than the mouse brain cell culture that we occasionally use (for transgenic animals only). Benito-Muñoz et al., Glia. 2016; Cavaliere et al., Front Cell Neurosci. 2013. It is true that there could be differences between the rat and mouse Thbs4-cell physiology, despite a 96% identity between rat and mouse Thbs4 protein sequence (BLASTp). In vitro, we only confirm the capacity of astrocytes to internalize hyaluronan, which was a finding that we did not expect in our in vivo experiments. Indeed, these observations, notwithstanding the obvious differences between in vivo and in vitro scenarios, suggest that the HA internalization by astrocytes is a cross-species event, at least in rodents. Regarding HA, hyaluronan is similar in all species, since it's a glycan (this is why there are no antibodies against HA, and ones has to rely on binding proteins such as HABP to label it).

> *(7) Similar comment for overexpression of naked mole rat HA.*

We chose the naked mole rat Hyaluronan synthase (HAS), because it is a HAS that produces HA of very high molecular weight, similar to the one found accumulated in the glial scar, at the lesion border. The naked-mole rat HAS used in mice (Gorbunova Lab) is a known tool in the ECM field. (Zhang et al, 2023, Nature; Tian et al., 2013, Nature).

> ***Reviewer 1 (Recommendation to authors):***
>
> *(1) Line 22: most of the cells that migrate out of the SVZ are not stem cells but cells further along in the lineage - neuroblasts and glioblasts.*

We thank the reviewer for this clarification. We have modified the abstract accordingly.

> *(2) In Figure 3d the MCAO group staining with GFAP looks suspiciously like ependymal cells which have been shown to be dramatically activated by stroke models.*

The picture does show ependymal cells, which are located next to the ventricle and are indeed very proliferative in stroke. However, these cells do not express Thbs4 (Shah et al., 2018, Cell). In the quantifications from the SVZ of BrdU and IdU injected animals (Fig 3e and f), we only take into account Thbs4+ GFAP+ cells, no GFAP+ only.

> *(3) The TTC injury shown in Figure 5c is too low mag.*

We apologize for the low mag. We have increased the magnification two-fold without compromising resolution. The problem might also have arisen from the compression of TIF into JPEG in the PDF export process. We will address this in the revised version by carefully selecting export settings. The images we used are all publication quality (300 ppi).

> *(4) How specific to HA is HABP?*

Hyaluronic Acid Binding Protein is a canonical marker for hyaluronan that is used also in ELISA to quantify it specifically, since it does not bind other glycosaminoglycans. The label has been used for years in the field for immunochemistry, and some controls and validations have been published: Deepa et al., 2006, JBC performed appropriate controls of HABP-biotin labeling using hyaluronidase (destroys labeling) and chondroitinase (preserves labeling). Soria et al., 2020, Nat Commun checked that (i) streptavidin does not label unspecifically, and (ii) that HABP staining is reduced after hyaluronan depletion in vivo with HAS inhibitor 4MU.

> *(5) A number of images are out of focus and thus difficult to interpret (e.g. SFig. 4e).*

This is true. We realized that the PDF conversion process for the preprint version has severely compressed the larger images, such as the one found in Fig. S4e. We have submitted a revised version in a better-quality PDF (the final paper will have the original TIFF files). We apologize for the technical problem.

> *(6) "restructuration" is not a word.*

We apologize for the mistake and thank the reviewer for the correction. We corrected “restructuration” with “reorganization” in line 67.

> *(7) While much of the manuscript is well-written and logical it could use an in-depth edit to remove awkward words and phrasings.*

A native English speaker has revised the manuscript to correct these awkward phrases. All changes are labeled in red in the revised version.

> *(8) Please describe why and how you used skeleton analysis for HABP in the methods, this will be unfamiliar to most readers. The one-sentence description in the methods is insufficient.*

We have modified the text accordingly, explaining in depth the logic behind the skeleton analysis. (Line 204). We also added several lines of text describing in detail the image analysis (CD44/HABP spots, fractal dimension, masks for membranal HABP, among others, in lines 484494)

> ***Reviewer #2 (Public Review)***
>
> *Summary:*
>
> *In their manuscript, Ardaya et al have addressed the impact of ischemia-induced gliogenesis from the adult SVZ and their effect on the remodeling of the extracellular matrix (ECM) in the glial scar. They use Thbs4, a marker previously identified to be expressed in astrocytes of the SVZ, to understand its role in ischemia-induced gliogenesis. First, the authors show that Thbs4 is expressed in the SVZ and that its expression levels increase upon ischemia. Next, they claim that ischemia induces the generation of newborn astrocyte from SVZ neural stem cells (NSCs), which migrate toward the ischemic regions to accumulate at the glial scar. Thbs4-expressing astrocytes are recruited to the lesion by Hyaluronan where they modulate ECM homeostasis.*
>
> *Strengths:*
>
> *The findings of these studies are in principle interesting and the experiments are in principle good.*
>
> *Weaknesses:*
>
> *The manuscript suffers from an evident lack of clarity and precision in regard to their findings and their interpretation.*

We thank the reviewer for the valuable feedback. We hope the changes proposed improve clarity and precision throughout the manuscript.

> *(1) The authors talk about Thbs4 expression in NSCs and astrocytes, but neither of both is shown in Figure 1, nor have they used cell type-specific markers.*

As we reported also to Referee #1 (major point 1), Thbs4 is widely considered in literature as a valid marker for newly formed astrocytes (Beckervordersanforth et al., 2010; Benner et al., 2013; Llorens-Bobadilla et al. 2015, Codega et al, 2014; Basak et al., 2018; Mizrak et al., 2019; Kjell et al., 2020; Cebrian-Silla et al., 2021). Some of the studies mentioned here and discussed in the manuscript text, also associate Thbs4 to B-type cells based on scRNAseq data (LlorensBobadilla et al. 2015; Cebrian-Silla et al., 2021; Basak et al., 2018). Moreover, we also showed colocalization of Thbs4 with activated stem cells marker nestin (Fig.2), glial marker GFAP (Fig. 3) and with dorsal NSCs marker tdTOM (from electroporation, Fig. 4).

> *(2) Very important for all following experiments is to show that Thbs4 is not expressed outside of the SVZ, specifically in the areas where the lesion will take place. If Thbs4 was expressed there, the conclusion that Thbs4+ cells come from the SVZ to migrate to the lesion would be entirely wrong.*

In Figure 1a, we show that Thbs4 is expressed in the telencephalon, exclusively in the neurogenic regions like SVZ, RMS and OB, together with cerebellum and VTA, which are likely not directly topographically connected to the damaged area (cortex and striatum). Regarding the origin of Thbs4+ cells, we demonstrated their SVZ origin by lineage tracking experiments after in vivo cell labeling (Fig. 4).

> *(3) Next, the authors want to confirm the expression level of Thbs4 by electroporation of pThbs4-eGFP at P1 and write that this results in 20% of total cells expressing GFP, especially in the rostral SVZ. I do not understand the benefit of this sentence. This may be a confirmation of expression, but it also shows that the GFP+ cells derive from early postnatal NSCs.*

> *Furthermore, these cells look all like astrocytes, so the authors could have made a point here that indeed early postnatal NSCs expressing Thbs4 generate astrocytes alongside development. Here, it would have been interesting to see how many of the GFP+ cells are still NSCs.*

We thank the reviewer for this useful remark. We have rephrased this paragraph in the results section (Line 99).

> *(4) In the next chapter, the authors show that Thbs4 increases in expression after brain injury. I do not understand the meaning of the graphs showing expression levels of distinct cell types of the neuronal lineage. Please specify why this is interesting and what to conclude from that.*

Also here, the expression of Thbs4 should be shown outside of the SVZ as well.

In Fig 2, we show the temporal expression of two markers (besides Thbs4) in the SVZ. Nestin and DCX are the gold standard markers for NSCs, with DCX present in neuroblasts. This is already explained in line 119. What we didn't explain, and now we say in line 124, is that Nestin and DCX decrease immediately after ischemia (7d time-point). This probably means that the NSCs stop differentiating into neuroblast to favor glioblast formation. This is also supported by the experiments in the olfactory bulb depicted in Fig. S5C-H.

> *(5) Next, the origin of newborn astrocytes from the SVZ upon ischemia is revealed. The graphs indicate that the authors perfused at different time points after tMCAO. Did they also show the data of the early time points? If only of the 30dpi, they should remove the additional time points indicated in the graph. In line 127 they talk about the origin of newborn astrocytes. Until now they have not even mentioned that new astrocytes are generated. Furthermore, the following sentences are imprecise: first they write that the number of slow proliferation NSCs is increased, then they talk about astrocytes. How exactly did they identify astrocytes and separate them from NSCs? Morphologically? Because both cell types express GFAP and Thbs4.*
>
> *The same problem also occurs throughout the next chapter.*

We thank the reviewer for this interesting comment. The experiment in Fig 3 combines BrdU and IdU. This is a tricky experiment, since chronic BrdU is normally analyzed after 30d, since the experimenter must wait for the wash out of BrdU (it labels slow-proliferating cells). Since we also wanted to label fast proliferative cells with IdU, we used IP injections of this nucleotide at the different time points, and perfused the day after. It wouldn't make sense to show BrdU at earlier time points. We do so in Fig 3e, just to colocalize with Thbs4 to read the tendency of the experiment. However, the quantification of BrdU (not of IdU) is done only at 30 DPI, which is explained in the methods (line 407).

> *"In line 127, they talk about the origin of newborn astrocytes…"*

Indeed, we wanted to introduce in the paragraph title that ischemia induced the generation of new astrocytes, which is more clearly described in the text. We changed the paragraph title with "Characterization of Ischemia-induced cell populations"

> *"How exactly did they identify astrocytes and separate them from NSC?"*

With this experiment and using two different protocols to label proliferating cells (BrdU vs IdU) we wanted to track the precursor cells that derivate to astrocytes and that already expressed the marker Thbs4. Indeed, the different increase and rate of proliferation is only

related to the progenitor cells that lately will differentiate in astrocytes. In this experiment we only referred to the astrocytes in the last sentence “These results suggest that, after ischemia, Thbs4positive astrocytes derive from the slow proliferative type B cells”

> *(6) "These results suggest that ischemia-induced astrogliogenesis in the SVZ occurs in type B cells from the dorsal region, and that these newborn Thbs4-positive astrocytes migrate to the ischemic areas." This sentence is a bit dangerous and bares at least one conceptual difficulty: if NSCs generate astrocytes under normal conditions and along the cause of postnatal development (which they do), then local astrocytes (expressing the tdTom because they stem from a postnatal NSC), may also react to MCAO and proliferate locally. So the astrocytes along the scar do not necessarily come from adult NSCs upon injury but from local astrocytes. If the authors state that NSCs generate astrocytes that migrate to the lesion, I would like to see that no astrocytes inside the striatum carry the tdTom reporter before MCAO is committed.*

We understand the referee’s concern about the postnatal origin of astrocytes that can also be labeled with tdTom. Our hypothesis, tested at the beginning of the paper, is that SVZ-derived astrocytes derive from slow proliferative NSC. Thus, it is reasonable that Tom+ cells can reach the cortical region in such a short time frame. This is why we assumed that local astrocytes can’t be positive for tdTom. We characterized the expression of tfTom in sham animals and we observed few tdTom+ cells in the cortex and striatum (Author response image 2 and Figure S4). The expression of tdTom mainly remains in the SVZ and the corpus callosum under physiological conditions. However, proliferation of local astrocytes labeled with tdTom expression (early postnatally astrocytes) could explain the small percentage of tdTom+ cells in the ischemic regions that do not express Thbs4, even though this percentage could represent other cell types such as OPCs or oligodendrocytes.

Author response image 2.

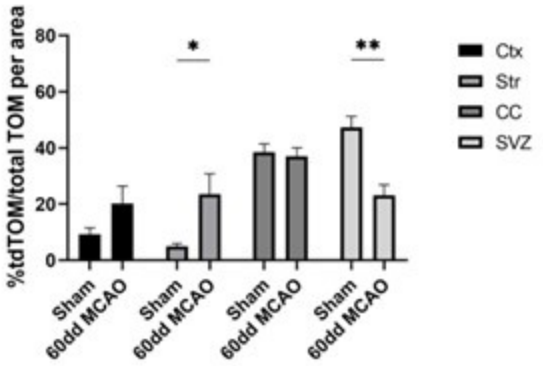

> *(7) If astrocytes outside the SVZ do not express Thbs4, I would like to see it. Otherwise, the discrimination of SVZ-derive GFAP+/Thbs4+ astrocytes and local astrocytes expressing only GFAP is shaky.*

Regarding Thbs4 outside the SVZ, we already answered this in point 2 (please refer to Fig 1A). We also quantified the expression of Thbs4+/GFAP+ astrocytes in the corpus callosum, cortex and striatum of sham and MCAO mice (Figure S5a-b) and we did not observe that local astrocytes express Thbs4 under physiological conditions.

> *(8) Please briefly explain what a Skeleton analysis and a Fractal dimension analysis is, and what it is good for.*

We apologized for the brief information on Skeleton and Fractal dimension analysis. We included a detailed explanation of these analyses in methods (line 484-494).

> *(9) The chapter on HA is again a bit difficult to follow. Please rewrite to clarify who produces HA and who removes it by again showing all astrocyte subtypes (GFAP+/Thbs4+ and GFAP+/Thbs4-).*

We apologize for the lack of clarity. We rewrote some passages of those chapters (changes in red), trying to convey the ideas more clearly. We also changed a panel in Figure S6b-c to clarify all astrocytes subtypes that internalize hyaluronan (Thbs4+/GFAP+ and Thbs4-/GFAP+). See Author response image 3.

Author response image 3.

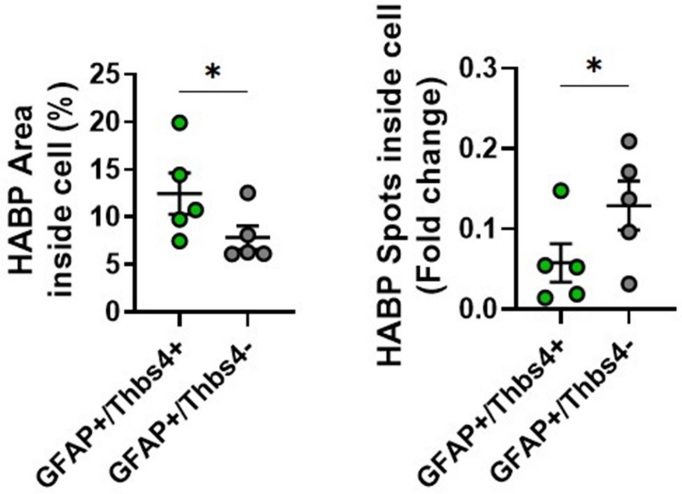

> *(10) Why did the authors separate dorsal, medial, and ventral SVZ so carefully? Do they comment on it? As far as I remember, astrogenesis in physiological conditions has some local preferences (dorsal?)*

We performed the electroporation protocol in the dorsal SVZ based on previous results (Figure 3 and Figure S3). NSC produce specific neurons in the olfactory bulb according to their location in the SVZ. However, postnatal production of astrocytes mainly occurs through local astrocytes proliferation and the SVZ contribution is very limited at this time point.

> ***Reviewer #3 (Public Review)***
>
> *Summary:*
>
> *The authors aimed to study the activation of gliogenesis and the role of newborn astrocytes in a post-ischemic scenario. Combining immunofluorescence, BrdU-tracing, and genetic cellular labelling, they tracked the migration of newborn astrocytes (expressing Thbs4) and found that Thbs4-positive astrocytes modulate the extracellular matrix at the lesion border by synthesis but also degradation of hyaluronan. Their results point to a relevant function of SVZ newborn astrocytes in the modulation of the glial scar after brain ischemia. This work's major strength is the fact that it is tackling the function of SVZ newborn astrocytes, whose role is undisclosed so far.*

Strengths:

The article is innovative, of good quality, and clearly written, with properly described Materials and Methods, data analysis, and presentation. In general, the methods are designed properly to answer the main question of the authors, being a major strength. Interpretation of the data is also in general well done, with results supporting the main conclusions of this article.

Weaknesses:

However, there are some points of this article that still need clarification to further improve this work.

(1) As a first general comment, is it possible that the increase in Thbs4-positive astrocytes can also happen locally close to the glia scar, through the proliferation of local astrocytes or even from local astrocytes at the SVZ? As it was shown in published articles most of the newborn astrocytes in the adult brain actually derive from proliferating astrocytes, and a smaller percentage is derived from NSCs. How can the authors rule out a contribution of local astrocytes to the increase of Thbs4-positive astrocytes? The authors also observed that only about one-third of the astrocytes in the glial scar derived from the SVZ.

We thank the reviewer for the interesting comment. We have extended the discussion about this topic in the manuscript, (lines 333-342), including the statement about a third of glial scar astrocytes being from the SVZ and not downplaying the role of local astrocytes. Whether the glial scar is populated by newborn astrocytes derived from SVZ or from local astrocytes is under debate, since there are groups that found astrocytes contribution from local astrocytes (Frisèn group, Magnusson et al., 2014) but there are others that observed the opposite (Li et al., 2010; Benner et al., 2013; Faiz et al., 2015; Laug et al., 2019 & Pous et al., 2020).

In our study we observed that Thbs4 expression is almost absent in the cortex and striatum of sham mice. To demonstrate that new-born astrocytes are derived from SVZ we used two techniques: the chronic BrdU treatment and the cell tracing which mainly labels SVZ neural stem cells. Fast proliferating cells lose BrdU quickly so local astrocytes under ischemic conditions do not express BrdU. In addition, we injected IdU the day before perfusion in order to see if local astrocytes express Thbs4 when they respond to the brain ischemia. However, we did not observe proliferating local astrocytes expressing Thbs4 after MCAO (see Author response image 4)

Author response image 4.

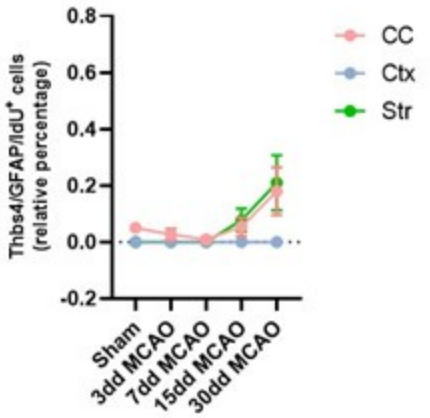

As mentioned in the response for reviewer 2, the cell tracing technique could label early postnatal astrocytes. We characterized the technique and only a small percentage of tdTom expression was found in the cortex and striatum of sham animals. This tdTom population could explain the percentage of tdTom+ cells in the ischemic regions that do not express Thbs4 even though this percentage could represent other cell types such as OPCs or oligodendrocytes. Taking all together, evidences suggest that Thbs4+ astrocyte population derived from the SVZ.

We indeed observed a small contribution of Thbs4+ astrocytes to the glial scar. However, Thbs4+ astrocytes arrive at the lesion at a critical temporal window - when local hyper-reactive astrocytes die or lose their function. We hypothesized that Thbs4+ astrocytes could help local astrocytes or replace them in reorganizing the extracellular space and the glial scar, an instrumental process for the recovery of the ischemic area.

> *(2) It is known that the local, GFAP-reactive astrocytes at the scar can form the required ECM. The authors propose a role of Thbs4-positive astrocytes in the modulation, and perhaps maintenance, of the ECM at the scar, thus participating in scar formation likewise. So, this means that the function of newborn astrocytes is only to help the local astrocytes in the scar formation and thus contribute to tissue regeneration. Why do we need specifically the Thbs4positive astrocytes migrating from the SVZ to help the local astrocytes? Can you discuss this further?*

Unfortunately, we could not demonstrate which molecular machinery is involved in these mechanisms, and we can only speculate the functional meaning of a second wave of glial activation. We added a lengthy discussion in lines 333-342.

> *(3) The authors observed that the number of BrdU- and DCX-positive cells decreased 15 dpi in all OB layers (Fig. S5). They further suggest that ischemia-induced a change in the neuroblasts ectopic migratory pathway, depriving the OB layers of the SVZ newborn neurons. Are the authors suggesting that these BrdU/DCX-positive cells now migrate also to the ischemic scar, or do they die? In fact, they see an increase in caspase-3 positive cells in the SVZ after ischemia, but they do not analyse which type of cells are dying. Alternatively, is there a change in the fate of the cells, and astrogliogenesis is increased at the expense of neurogenesis? The authors should understand which cells are Cleaved-caspase-3 positive at the SVZ and clarify if there is a change in cell fate. Also please*

> *clarify what happens to the BrdU/DCX-positive cells that are born at the SVZ but do not migrate properly to the OB layers.*

Actually, we cannot demonstrate the fate of missing BrdU/DCX cells in the OB. We can reasonably speculate that following the ischemic insult, the neurogenic machinery steers toward investing more energy in generating glial cells to support the lesion. We didn't analyze the fate of the DCX that originally should migrate and differentiate to the OB, whether they die or if there is a shift in the differentiation program in the SVZ, since we consider that question is out of the study's scope.

> *(4) The authors showed decreased Nestin protein levels at 15 dpi by western blot and immunostaining shows a decrease already at 7div (Figure 2). These results mean that there is at least a transient depletion of NSCs due to the promotion of astrogliogenesis. However, the authors show that at 30dpi there is an increase of slow proliferating NSCs (Figure 3). Does this mean, that there is a reestablishment of the SVZ cytogenic process? How does it happen, more specifically, how NSCs number is promoted at 30dpi? Please explain how are the NSCs modulated throughout time after ischemia induction and its impact on the cytogenic process.*

Based on the chronic BrdU treatment, results suggested a restoration of SVZ cytogenic process (also observed in the nestin and DCX proteins expression at 30dpi). However, we did not analyze how it happens (from asymmetric or symmetric divisions). As suggested by Encinas group, we hypothesized that the brain ischemia induces the exhaustion of the neurogenic niche of the SVZ by symmetric divisions of NSC into reactive astrocytes.

> *(5) The authors performed a classification of Thbs4-positive cells in the SVZ according to their morphology. This should be confirmed with markers expressed by each of the cell subtypes.*

We thank the referee for the comment. Classifying NSC based on different markers could also be tricky because different NSC cell types share markers. This classification was made considering the specific morphology of each NSC cell type. In addition, Thbs4 expression in Btype cells is also observed in other studies (Llorens-Bobadilla et al. 2015; Cebrian-Silla et al., 2021; Basak et al., 2018).

> *(6) In Figure S6, the authors quantified HABP spots inside Thbs4-positive astrocytes. Please show a higher magnification picture to show how this quantification was done.*

We quantified HABP area and HABP spots inside Thbs4+ astrocytes with a custom FIJI script.

Thbs4 cell mask was done via automatic thresholding within the GFAP cell mask. Threshold for HABP marker was performed and binary image was processed with 1 pixel median filter (to eliminate 1 px noise-related spots). "Analyze particles" tool was used to sort HABP spots in the cell ROI. HABP spot number per compartment and population was exported to excel and data was normalized dividing HABP spots per ROI by total HABP spots. See Author response image 5.

Author response image 5.

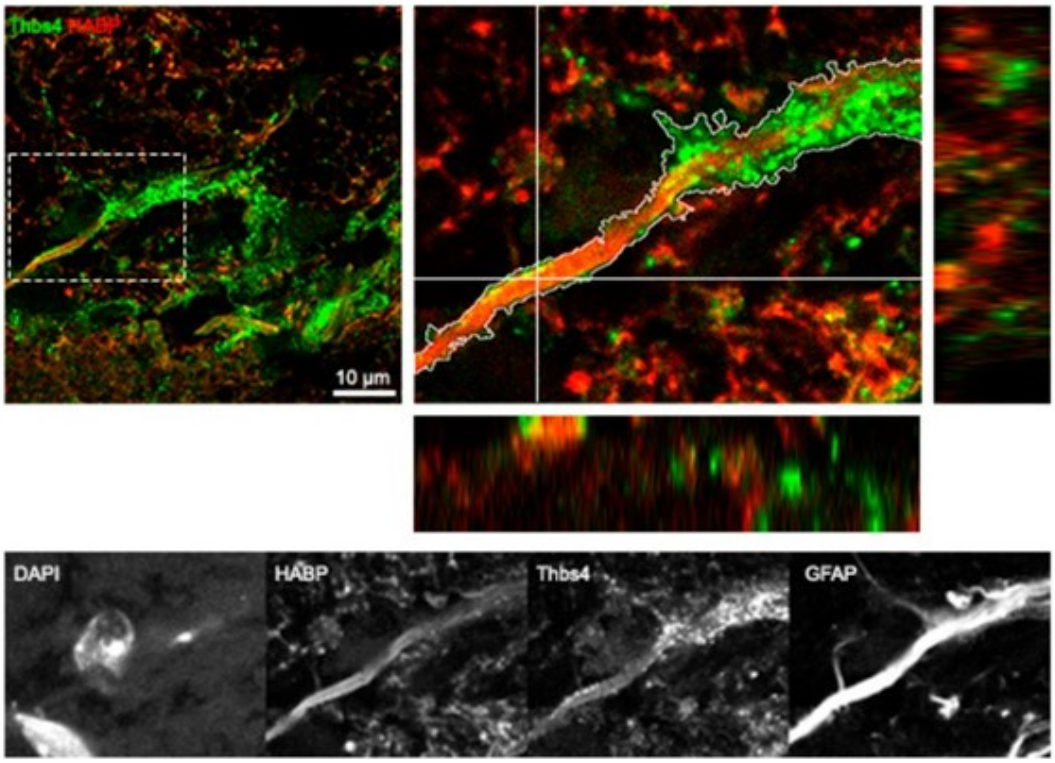

https://doi.org/10.7554/eLife.96076.2.sa0